Session A3

Inspection Methods and Monitoring
Méthodes d'inspection et de surveillance
Methoden für Inspektion und Ueberwachung

Leere Seite

Blank page

Page vide

Sonic Tomography Analysis of Concrete Structures
Analyse des structures de béton par tomographie sonique
Sonisch-tomographische Analyse von Betonbauwerken

Jamal RHAZI
Research Associate
University of Sherbrooke
Sherbrooke, PQ, Canada

Yahya KHARRAT
Civil Engineer
University of Sherbrooke
Sherbrooke, PQ, Canada

Gérard BALLIVY
Professor
University of Sherbrooke
Sherbrooke, PQ, Canada

Jamal Rhazi is a research associate in the Civil Engineering Department at the University of Sherbrooke, Canada. His research interests include instrumentation and non-destructive testing of concrete structures.

Yahya Kharrat has received an M.Sc degree in civil engineering at the University of Sherbrooke, Canada. He is currently pursuing a Ph.D. degree on sonic tomography.

Gérard Ballivy is a professor at Sherbrooke, Canada, since 1976. His main fields of interest are the auscultation and instrumentation of concrete structures and the design of grout products.

SUMMARY

This paper discusses theoretical as well as practical aspects of a relatively new process in civil engineering that can be used to visualize the internal condition of a concrete structure using non-intrusive data acquisition techniques. This process combines computer tomography of sonic data with scientific visualisation techniques. The resulting output is a representation of the structure showing the spatial distribution of stress wave velocity within the structure.

RÉSUMÉ

Cet article discute l'aspect théorique aussi bien que l'aspect pratique d'un nouveau procédé en génie civil qui permet la visualisation des conditions internes des structures en béton à partir de données collectées d'une manière non destructive. Ce procédé combine le calcul tomographique de données d'essais soniques aux techniques de visualisation scientifiques récentes. Le résultat est une représentation graphique indiquant la distribution spatiale de la vitesse sonique au sein de la structure.

ZUSAMMENFASSUNG

Diskutiert werden in diesem Artikel die theoretischen sowie die praktischen Aspekte eines neuen Verfahrens im Bauwesen, wodurch eine Visualisierung der inneren Bedingungen eines Betonbauwerkes möglich ist, ohne das Bauwerk zu zerstören. Dieses Verfahren ist eine Kombination von sonisch-tomographischen Berechnungen und der neuesten Kenntnisse in wissenschaftlicher Visualisierungstechnik. Das Ergebnis ist eine graphische Darstellung der Raumverteilung von sonischer Geschwindigkeit innerhalb eines Bauwerkes.

1. INTRODUCTION

Currently, the inspection of concrete structures relies on the visual examination of the exposed concrete surface, occasionally supported by a number of nondestructive tests and by the removal of core samples for laboratory testing. Such an approach is clearly limited if more detailed analysis of the concrete is required for service life predictions, safety assessement, rehabilitation programs or determination of the extent of deterioration throughout the structure.

This paper discusses theoretical and practical aspects of a relatively new process in civil engineering that can be used to visualize the internal condition of a concrete structure using non-intrusive data acquisition techniques. This process combines computer tomography of sonic data with scientific visualisation techniques. The resulting output is a representation of the structure showing the spatial distribution of stress wave velocity within the structure.

2. THEORETICAL ASPECT OF SONIC TOMOGRAPHY

As any other nondestructive technique, sonic tomography includes three steps: (1) the collection of data, (2) processing of the collected data, and (3) the analysis of the results.

The collection of data consists on propagating acoustical waves through the medium from the sources (hammer, air gun, explosive) to the receiver (piezoelectric sensors, accelerometers, geophones or hydrophones). The location of both the source and receiver must vary such so that waves can widely cover the surveyed section, uniformly and in a large number of directions [1]. In this way, it is possible to get a sufficient group of data (N) from the records of impulse waves to describe adequally the internal condition of the medium. For instance, travel times of longitudinal waves are the most information used to reconstruct the cross sectional velocity distribution. This choice is justified by the fact that velocity is related to the modulus and density, and hence indirectly to the srenght of concrete.

The next step of data processing consists in dividing the surveyed section into cells; the number of cells (P) that is produced should be fewer than the number of observed travel times data (N). The measured travel times are inverted by solving the equation:

$$G \cdot m = T \qquad (1)$$

T is a vector which each component t_i represents the travel time of the ith ray path $(1 < i < N)$. m is a vector that describes the distribution of the slowness in the medium defined as the inverse of velocity $(m_j, 1 < j < P)$ and G is a P x N matrix which each term g_{ij} is equal to the distance travelled by the ith ray path in the jth cell.

In practice, equation (1) is solved by inverting G and multiplying it with measured data given by T. However, the matrix G is often spare, large and singular [2]. Consequently, the system of equation is either undertermined or overdetermined. Many methods have been developed to estimate a matrix H that satisfies the equation:

$$m = H \cdot T \qquad (2)$$

Such methods are the algebric reconstruction technique (ART, [3]) and the simultaneous iterative reconstruction technique (SIRT, [4]).

In practice, an initial slowness model is determined from the known information on the medium. In the absence of any information, a special algorithm built an homogeneous model and the theoretical travel times of all source-receiver pairs are computed using a ray tracing method. The slowness values in the cells are adjusted to optimize the difference between measured and computed times. The slowness model is modified until the residual becomes acceptable and the final solution obtained.

3. EXAMPLES OF APPLICATION

Tomography measurements were conducted by capturing acoustical waves with a set of six accelerometers working in the frequency domain 1 - 15 KHz. The amplified and filtered signals were fed into a 6-channel data acquisition and recording system. In this manner, the medium response is detected at five different locations for a given source location, one sensor being fixed near the source to get the time zero reference.

Travel times measurements for each source-receiver pair were determined manually at a later time. The iterative algorithm was a SIRT type developed at the Laboratoire Central des Ponts et Chaussées (France) [5] and the back projection technique (BPT) was used for determination of the initial slowness model.

3.1   Diagnosis of a pile

The following example is an interesting one that shows both the effect of cracks and the quality of the concrete on the spatial distribution of the velocity.

Tomography measurements were performed on a 1-m diameter and 0.70-m depth cylindrical pile composed of three concentric cement-based mediums of different mechanical properties (Fig. 1). Before the test, several lateral fractures were induced in the pile by submitting the central medium to a hydraulic compressive stress. Figure 1 shows the cracks cartography as observed from the top of the pile.

1 Concrete
   E=18 GPa
   v = 0.19
   C0 = 25 MPA

2 Mortar
   E = 9 GPa
   v =0.17
   C0 =24 MPa

3 Concrete
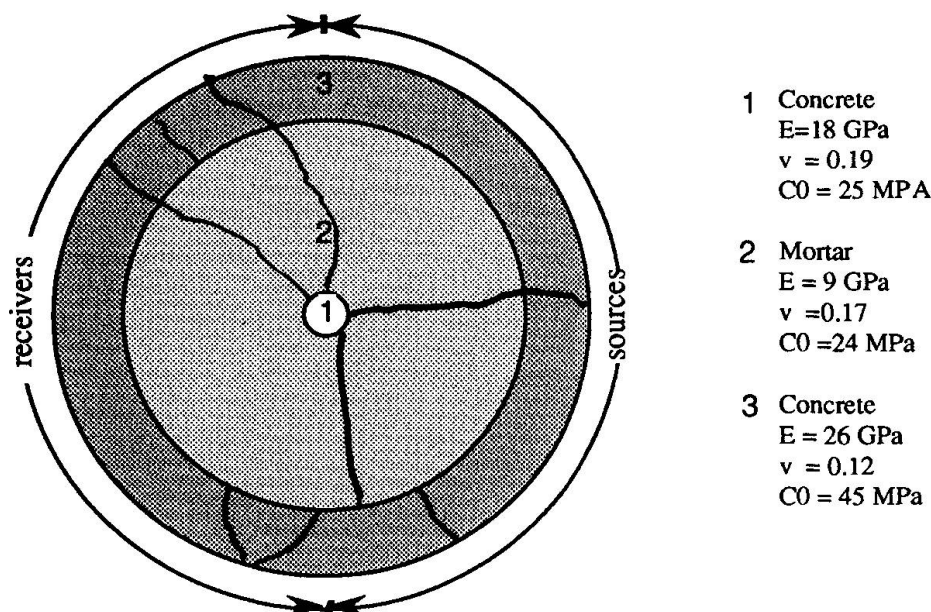   E = 26 GPa
   v = 0.12
   C0 = 45 MPa

Fig.1 Schematic drawing of the pile with crack cartography and the source-receiver geometry

In the case of this experiment, the best signal to noise ratio was obtained by the impact of a steel ball that has 8 mm diameter. The source-receiver geometry (Fig. 1) was chosen so that ray paths cover uniformly and sufficiently the surveyed section located at 0.30 m from the top of the pile. The distance between two successive emissions and two adjacent receivers were fixed to 0.1 m, resulting in a total of 324 data records (Fig. 2a).

The final velocity distribution indicated on figure 2b globally accounts for the composite nature of the pile:

- the central area is clearly identified and is described by a velocity varying between 4250 and 4 500 m/s,

- the mortar that fills 60% of the surveyed section has a lower velocity (3 750 to 4 000 m/s),

- the peripherical area has a velocity higher than 4 500 m/s.

The mortar - peripherical area boundary is however not regular. In particular, a low velocity (2 500 to 3 000 m/s) exists at the upper left, the middle right and the bottom of the image. Figure 1 shows that these areas are a cracked ones. The cracks are not visible in the image just as they are, but there presence induce a perturbation of the velocity field. Supplementary investigations indicated that the importance of these perturbations are more dependent upon the cracks density, the wave propagation mode (straight or curve) than the the measure density. On the other hand, velocity values at these areas are related to the depth of cracks: deeply is a crack, lower is the velocity value.
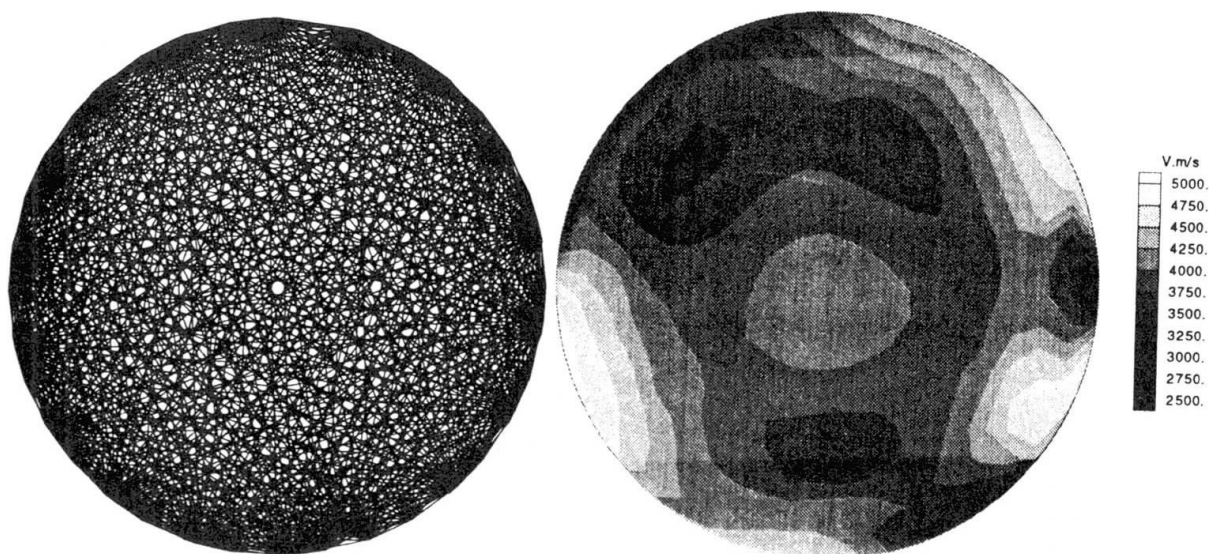

Fig.2a Ray diagram

Fig.2b Reconstructed velocity distribution image

3.2 Diagnosis of a pillar

This example illustrate results given by sonic tomography survey recently performed at a pillar of a concrete dam constructed in the 1920's. This pillar has the form of a gravity wall of 20 m in height, 3 m in thickness, and nearly 17 m in width at the bottom. The downstream face of the pillar

has been repaired some years ago due to a superficial degradation of the concrete in consequence of the long-term effect of hard climatic condition. Repair consisted of removing the damaged concrete and applying shotcrete. Core samples of 1-m long extracted perpendicularly to this face at four differents elevations (Fig. 3a) indicated that the thickness of shotcrete vary between 0.25 m and 0.40 m, and that the maximum aggregate size of new and old concrete are 20 mm and 50 mm respectively. The cores also indicate the presence of steel reinforcement of 20 mm in diameter.

A vertical section of the pillar was choosen to perform sonic measurements (figure 3a). Acoustical waves were generated by explosive. An existant filled water borehole along the upstream face was used to lower the source which we moved at 1-m intervals along the depth of concrete. The group of five receivers were placed along the downstream side for each source position. This procedure was repeated at three differents elevations of receivers; in this way, 225 travel times along crossing path with different inclinaisons were obtained. Figure 3b shows the final velocity model expressed by assigning the velocity values to each cell 1 m on side. Where ray density is low, reliability is probably poor, but tomographic image of the area gives sufficient informations. In particular, the image points out that the concrete is of two distinct qualities: poor-doubtful (2000 < V < 3600 m/s) and good-excellent (3600 < V < 4500 m/s), and that the concrete quality increases with depth.

The low velocity area on the top of downstream face reveals the extent of a damaged concrete visible from the outside, while the one on the upstream face coincides with the tidal zone. The interface between old and new concrete is however not visible on the image. This is probably due to a lack of data records on the downstream face (source and receivers on the donwstream face). Neverthless, laboratory tests on concrete samples show a good correlation among resistance values, elastic moduli and velocities (Table 1).
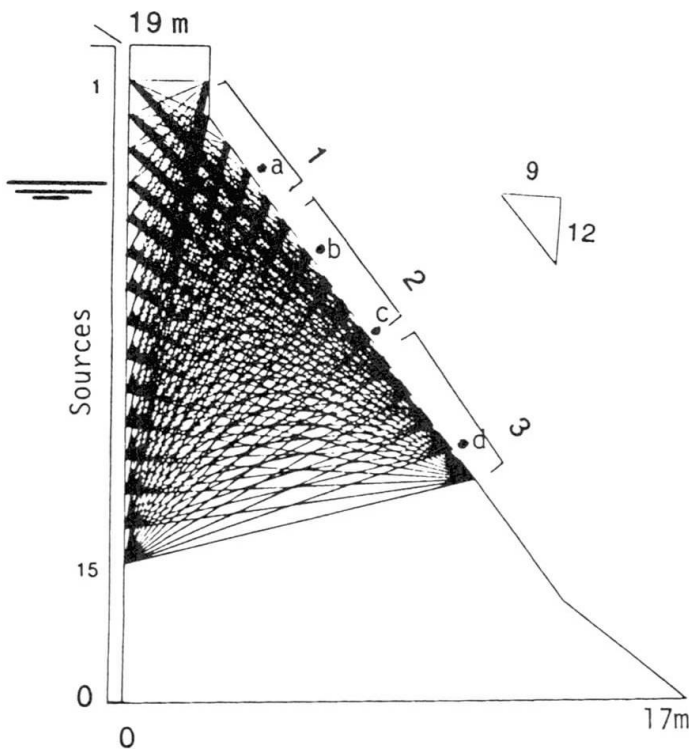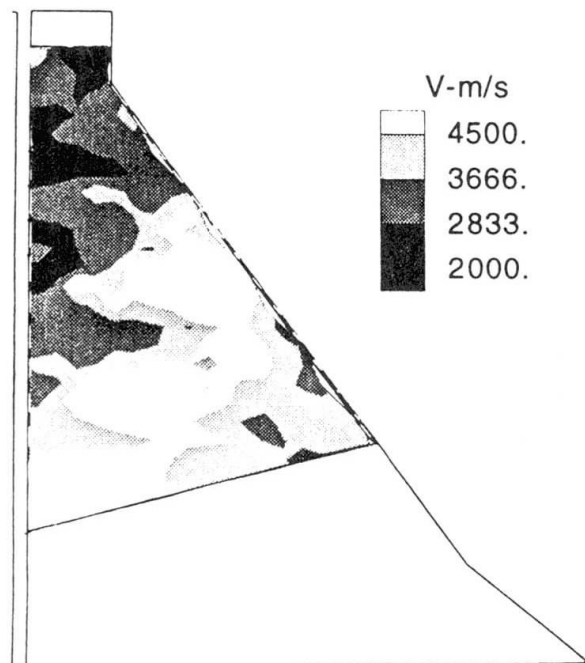

Fig.3a Scheme of measurements
(• position of boring)

Fig.3b Distribution of sonic
velocity.

Drilling N°	a	b	c	d
E (GPa)	14	24	19	21
C0 (MPa)	18	39	30	26

Table 1 Mean mechanical properties of core samples extracted from the downstream face

3 CONCLUSION

This paper has covered theoretical and practical aspects of sonic tomography. This nondestructive method is reliable, rapid and not very expensive and seems to be effective in evaluating the elastic dynamic characteristics of concrete and the state of intergrety of civil engineering structures. Recent application on a maconery structure has also shown that this technique'can be used as a cheking tool of the effectiveness of grouting work.

Obviously, sonic tomography can be improved. A solution that the authors are exploring is to consider wave attenuation inside the section of the structure examined. This information will permit to better define the concrete quality by a better location of the fractured areas

AKNOWLEDGEMENTS

REFERENCES

1. WORTHINGTON M.H., An Introduction to Geophysical Tomography. Oxford (U.K.), November 1984.

2. BERGMAN N.D., Tomographic Inversion of Crossehole Seismic Data. Research in Applied Geophysics. Vol 39, 1986.

3. GORDON R., A Tutorial on ART. IEEE Transactions on Nuclear Science, NS-21, 1974.

4. GILBERT P., Iterative Methods for the Reconstruction of Three-Dimensional Objects from Projection. Journal of Theoretical Biology, vol 36, 1972.

5. COTE Ph., Tomographie Sismique en Génie Civil. PhD thesis, Grenoble (France), 1988.

Checking Concrete by Quantitative Ultrasonics
Contrôle du béton par la méthode quantitative par ultrasons
Betonüberprüfung durch quantitativen Ultraschall

Ulrika WIBERG
Dr. Techn.
Vattenfall Utveckling AB
Alvkarleby, Sweden

Ulrika Wiberg, born in 1961, received her MSc. at the Royal Institute of Technology, Stockholm. She did research in ultrasonic testing and received her doctorate degree in 1994 at the Royal Institute of Technology. She is now working with condition assessment at a R&D company.

SUMMARY

Echo detection and tracking of deterioration in concrete is shown using quantitative ultrasonics. The method and analysis is described, and the difference from conventional ultrasonic testing is explained. The randomly scattered ultrasonic waves resulting from the composite are used for material characterisation purposes, and their influence is reduced by signal processing for echo detection. Several possible applications for checking concrete structures are indicated. Characterisation of micro-cracking can be performed using direct transmission. Voids and inclusions can be detected with direct transmission, and also in single-sided measurements if they cause echoes with other frequency characteristics than the material noise.

RÉSUMÉ

La méthode quantitative par ultrasons est appliquée pour la détection de la détérioration du béton. La méthode et l'analyse sont décrites et la différence, par rapport aux méthodes ultrasoniques conventionnelles d'essai, clarifiée. Les vagues ultrasoniques sont utilisées pour déterminer les caractéristiques du matériau. Plusieurs domaines d'application possibles pour l'emploi de la méthode quantitative par ultrasons dans le contrôle de structures en béton sont indiqués. La définition des micro-craquelures peut être effectuée en utilisant une transmission directe. Vides et inclusions peuvent être détectés par transmission directe et par mesures individuelles.

ZUSAMMENFASSUNG

Echoortung und die Verfolgung von Alterungen im Beton werden durch die Verwendung von quantitativem Ultraschall gezeigt. Verfahren und Analyse werden beschrieben und der Unterschied zur herkömmlichen Ultraschallprüfung wird erklärt. Die beliebig zerstreuten Ultraschallwellen, die vom Verbundmaterial stammen, werden für die Materialkennzeichnung verwendet und ihr Einfluss wird durch Signalverarbeitung für Echoortung reduziert. Mehrere mögliche Anwendungen für den Gebrauch von QU bei der Prüfung von Betonstrukturen werden aufgezeigt. Die Kennzeichnung der Mikrorissbildung kann durch Direktübertragung ausgeführt werden. Hohlräume und Einschlüsse können bei Direktübertragung wie auch bei einseitigen Massnahmen entdeckt werden.

1. BACKGROUND

To assess the condition of an existing concrete structure, defects must be detected and the state of the material must be determined. Concrete exposed to deteriorating processes will change its properties, and these changes need to be characterised prior to determining the state of health. Evaluation techniques are needed for the detection of distinct defects such as cracks and delaminations as well as for tracking the distributed damage caused by deterioration.

Methods based on ultrasonic wave propagation are interesting for these purposes. New measurement technique is developed and new methods for analysing ultrasonic data is used in concrete testing. Some of the more recent advances include ultrasonic pulse-echo measurement equipment [1][4], and data processing adopted to handle the composite nature of concrete [5]. Other new applications are in the field of material characterisation using spectroscopy [2][3][5].

2. QUANTITATIVE ULTRASONICS - METHOD AND ANALYSIS

Ultrasonic waves propagating in concrete are likely to be affected by the composite structure of the material, at least at high frequencies. These are random effects which might lead to misinterpretations as false echoes or reproducibility problems in conventional ultrasonics, viewing the signal as coming from a homogeneous medium. However, if such effects of the material character are present in a captured wave form, it carries an imprint of the state of the material. NDT using pulsed ultrasonic waves is expected to give a total measured response which contains both direct specular waves and randomly scattered waves since the pulses include a broad band of frequencies. The specular waves which arrive coherently in frequency can be modelled. The randomly scattered waves which appear incoherently in space and frequency are difficult to model.
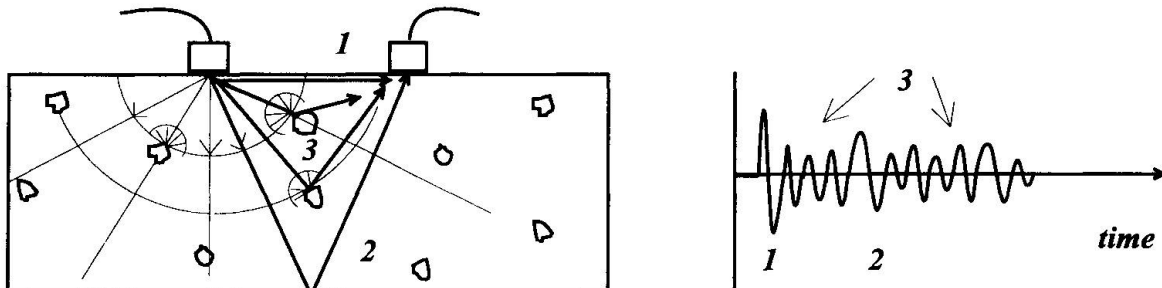

Fig. 1 Schematic representation of waves propagating in a heterogeneous solid

Methods to either analyse the scattered part of the wave form for material characterisation, or to reduce this influence to be able to identify echoes can be useful as true ultrasonic waves are likely to be scattered in concrete. Flaws large enough to cause specular echoes might be detected from the total wave form if the coherent waves are enhanced so that they are distinguished from the scattered waves. This could be achieved by substantial spatial averaging to reduce the random parts of the wave form, or by simply low pass filtering to reduce high frequency scattering. The first of these procedures requires many signals from comparable measurement locations and is thus not suitable for field applications. The other one uses a single record, but is likely to leave some of the scatter and will produce longer echoes thus reducing the resolution of echoes. Another possibility is to use the frequency dependence of the scattered waves to average them out. For the purpose of enhancing specular waves a split spectrum processing technique was tried which preserves or even improves the resolution.

The scattered waves are expected to carry information about the concrete composition, state of deterioration and defects cutting off direct specular waves. The material through which the wave is propagated acts as a frequency filter on the wave form. The material character was investigated using spectral measures reflecting the frequency shift in the received signal due to scattering.

Estimation of filtering characteristics can be done with fourier methods, or as was done in this investigation with parametric modelling using auto regressive low order models from which resonating frequencies can be estimated. The effect of scattering in a measured wave form can be examined by averaging the power of signals. Coarse grains and long transmission paths increase the scattering effect possibly making it a dominating feature in the measured wave form. The diffused behaviour of scattered waves can be analysed by forming the average power called the pulse shape.

3. MATERIAL CHARACTERISATION AND TRACKING OF INTRINSIC DAMAGE

Quantitative ultrasonics was used in this investigation to verify the presence of scattered waves in concrete, and for determining the extent of material deterioration. The results from measurements in deteriorated concrete showed that the additional attenuation, due to deterioration can be used to characterise the degree of deterioration.

3.1 Scattering in sound concrete

The effect of grain noise was investigated by measurements on two concrete slabs with different maximal grain sizes. Echo measurements with a two transducer arrangement were made on two slabs with thicknesses 0.10 m, one with fine grains (< 0.5mm) and the other with coarser grains (<18mm). The measurements were made with a transducer spacing of twice the slab thickness. The echo signal clearly shows substantial grain noise in the coarse grained concrete (fig.2). The bottom echo at 114 μs can be identified only in the fine grained material.
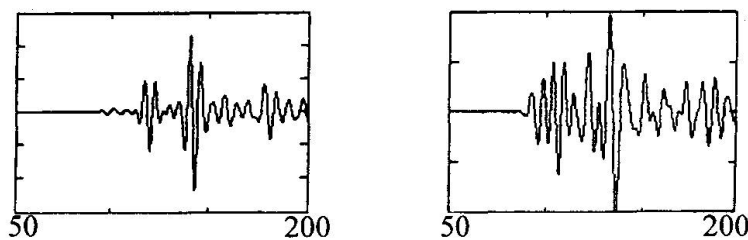

Fig. 2. Measured echo signals from a fine and a coarse grained concrete versus time [μs]

Frequency dependent attenuation of broad band pulses in concrete was shown, and the scattering effect was shown to increase with increasing travel paths in direct transmission measurements. The frequency filtering of measured signals due to the material causes power spectral changes. Spectral estimates of the first few oscillations of signals transmitted over path lengths 0.10, 0.35 and 0.50 m shifts towards lower frequencies for longer transmission paths (fig.3). A similar effect was shown comparing fourier spectra from slabs with fine and coarse grains.
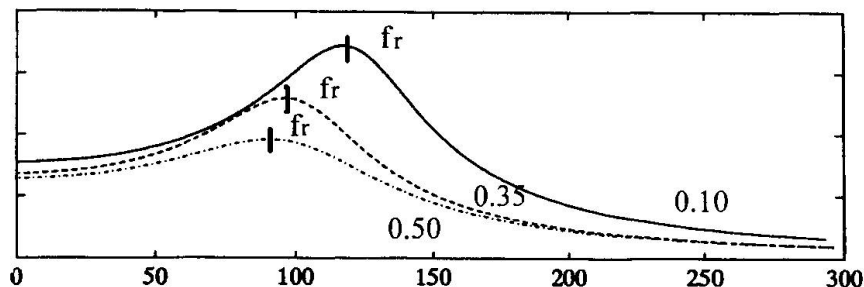

Fig. 3. Spectral estimates versus frequency [kHz] from path lengths 0.10, 0.35 and 0.50 m

3.2 Crack detection

The ultrasonic signal was shown to be sensitive to deterioration causing cracking, and thus quantitative measures from the signal can be used to track deterioration.
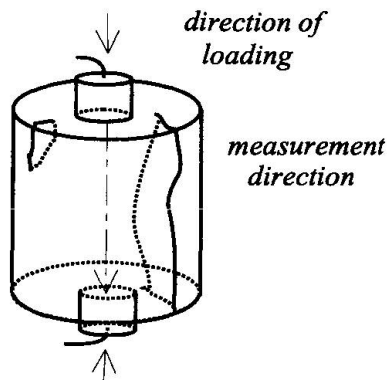
Fig. 4. Ultrasonic testing of a cracked concrete cylinder

A total of 18 cored concrete cylinders with height and diameter 0.10m were exposed to cyclic loads in the axial direction. The load was introduced as a sinusoidal pressure varying from almost zero to a maximum value specific for each specimen as described in [5]. The stage of deterioration was characterised by investigation of the development of cracks. All cracks visible on the surfaces of the cylinders were registered. A normalised amount of cracks λ was defined as the summed crack length divided by the cylinder height. The closeness to failure expressed as the ratio between the number of applied load cycles and the number of cycles at failure N/Nf was also used to characterise the deterioration for six specimens that were loaded to failure.

The degree of deterioration was investigated using various quantitative ultrasonic spectral measures such as resonating frequency fr estimated by parametric modelling of the first few cycles of the pulse (fig. 5). It was shown that the frequency dependent attenuation tracked crack growth rather than closeness to failure.
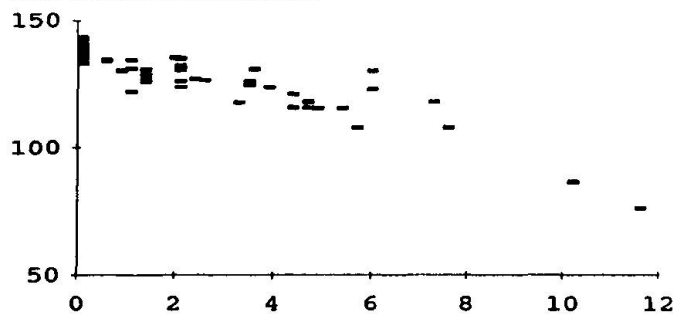
Fig. 5. Resonating frequency fr [kHz] versus normalised amount of cracks λ

3.3 Detection of freeze-thaw deterioration

Quantitative ultrasonics was shown to track internal crack growth due to freezing and thawing.
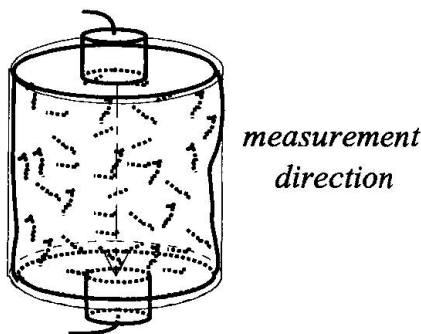
Fig. 6. Ultrasonic testing of a freeze-thaw deteriorated cylinder

Nine groups of concrete cylinders with three specimens in each group were exposed to 0, 1, 7, 14 or 28 cycles of freezing and thawing; half of them in contact with chlorides. Scaling reduced the cross sections and heights of the specimens especially for specimens frozen with chlorides. For the ultrasonic investigation the top and bottom surfaces of the specimens were therefore ground resulting in heights varying between 0.08 and 0.10 m. The effect of deterioration was evaluated from changing material properties characterised by strength and stiffness of the central parts of the cylinders. Internal cracking and surface scaling were also evaluated [5].

Fig. 7. Squared values of measured ultrasonic velocities [(km/s)] versus stiffness K [GPa]

Ultrasonic velocity as well as spectral changes were shown to mainly follow the number of freeze-thaw cycles, roughly reflecting internal crack growth. Quantitative ultrasonic measures to some extent also reflect changes in strength and stiffness. but not so that stiffness can be estimated from measured velocity (fig. 7), at least not without prior knowledge of the possible changes in Poisson's ratio due to deterioration. A comparison of relationships between s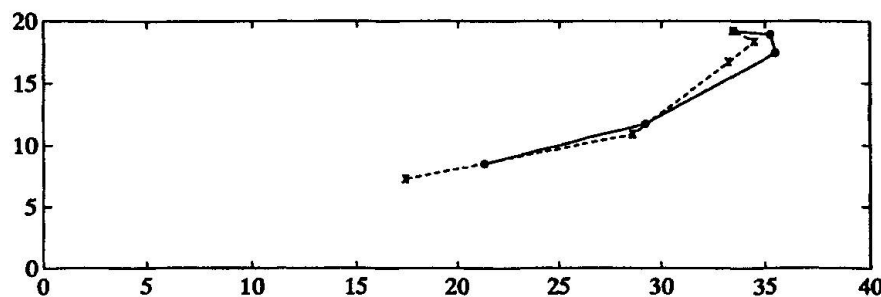trength and velocity, for deteriorated and undeteriorated concrete showed that the ultrasonic velocity decreased more rapidly with deterioration than was explained by the decrease in compressive strength.

4. DEFECT DETECTION IN STRUCTURES

Pulse-Echo measurements from concrete were shown to contain back scattered material noise with a clear frequency dependence. The frequency dependent character was used successfully to reduce the clutter, thus enhancing the coherently repeated specular echoes. The forward scattered energy was used in order to identify the presence of voids in a direct transmission measurement.

Echo measurements on concrete plates with thicknesses 0.10, 0.20, 0.30 m were made with broad band focused transducers. The measured signals were band pass filtered for evaluation of coherent specular signals and incoherent scattered waves. The measured response from the 0.30 m slab was the only one that showed a clear bottom echo in the low frequency part of the signal (fig.8).
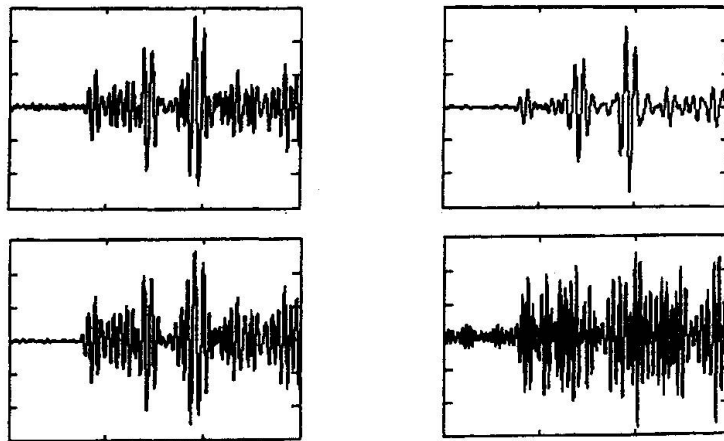
Fig. 8. a) Measured random signal from a slab with thickness 0.30 m. Band pass filtered signals with centre frequencies b) 75 kHz, c) 150 kHz and d) 225 kHz.

Split spectrum processing was used to reduce material noise from single sample records thus enabling identification of specular echoes with good resolution. The signal from the 0.30 m thick slab (fig 8a) showed a clear echo after split spectrum processing (fig 9) as did the signal from the 20 cm slab. The echo in the signal from the 0.10 m slab could not be clearly identified.

150   250   350

Fig. 9. Echo signal after Split Spectrum Processing versus time t [μs].

Total pulse shapes from direct transmission measurements were used to illustrate defect detection using forward scattered information. The absence of a distinct direct wave being replaced by a diffused arrival of waves indicates that a defect is cutting off the direct travel path. Total pulse shapes were formed by short time averaging of the power of measured signals and subsequent spatial averaging of the power signals from eight comparable locations. Measurements were made

on a concrete slab with thickness 0.31 m with plastic tubes embedded in the concrete. Three tubes with diameter 0.11 m were placed at various depths in the concrete, and five tubes with diameter 0.04 m were placed the same way. The concrete had maximal aggregate size 0.032 m which is close to the size of the small tubes. Total pulse shapes from a solid section, from a 0.11m tube in the middle of the slab, and from a 0.04m tube in the middle of the slab showed that the larger tube causes a diffused arrival of waves whereas the small tube appears in a way similar to the solid section (fig 10). All three large tubes appeared in a similar way, and so did all the small tubes.
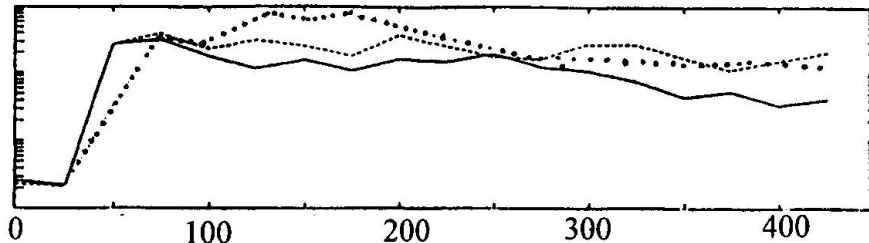

Fig 10. Total pulse shape versus time t [μs] for solid concrete (solid line), section with small tube (dashed line) and section with large tube (dotted line)

5. CONCLUSIONS

Ultrasonic waves in concrete were shown to contain incoherently scattered as well as coherent specular waves. It was shown that the frequency dependence of scattered waves can be used for material characterisation purposes, and that scattered waves can be used for defect detection.

Ultrasonic measurements on freeze-thaw deteriorated specimens, as well as measurements on specimens subjected to cyclic loads, showed that the quantitative ultrasonic measures mainly tracked crack growth. Strength, stiffness or closeness to failure were not significantly related to the ultrasonic measures in the cases presented here. The possible use of scattered waves for defect detection was verified. A total pulse shape with a diffused arrival of forward scattered waves was shown in a direct transmission measurement passing a 0.1 m tube. Echo detection in concrete using split spectrum processing to reduce material noise in measured signals was shown. Bottom echoes from slabs with thicknesses 0.20 and 0.30 m were identified with very good resolution.

ACKNOWLEDGEMENT

REFERENCES

1. Alexander, A.M., Thornton, H.T., Developments in Ultrasonic Pitch-Catch and Pulse-Echo for measurements in Concrete, ACI Special Publication, SP-112, pp.21-40, 1988.

2. Berthaud, Y., Damage Measurements in Concrete via an Ultrasonic Technique, Cement and Concrete Research, Vol.21, pp. 73-82, 1991.

3. Daponte, P., Olivito, R., Frequency Analysis for Crack Detection in Concrete, Proc. 9th Int. Conf. on Exp. Mechanics, Copenhagen, pp.1355-1364, 1990.

4. Tasker, C.G., Milne, J.M., Smith, R.L., Recent work at the national NDT centre on Concrete Inspection, Br.J. of NDT, Vol.32, pp. 355-359, 1990.

5. Wiberg, U., Material Characterization and Defect Detection in Concrete by QU, TRITA-BKN. Bulletin 7, Royal Institute of Technology, Department of Structural Engineering, Stockholm, 1993.

Radar Inspection of Structures
Inspection par radar des structures
Radaruntersuchung von Bauwerken

Stuart MATTHEWS
Head, Struct. Appraisal Section
Building Research Establishment
Garston, United Kingdom

S. Matthews graduated in 1973 and received his doctorate in 1978. He worked on the design and construction of public works, then in a testing house and in a consulting firm. In 1992 Dr Matthews joined BRE to undertake research in structural appraisal & monitoring techniques.

Frederick TSUI
Higher Scientific Officer
Building Research Establishment
Garston, United Kingdom
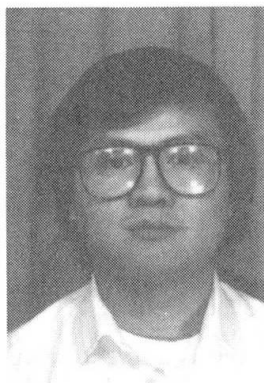
Frederick Tsui, born 1958, obtained his degree at Middlesex Univ. He attended a postgraduate course at Imperial College, and undertook research work there until he joined BRE in 1994. His research interests are in artificial intelligence and numerical modelling of structures.

SUMMARY

Subsurface radar is being used increasingly during the investigation and appraisal of a wide range of existing buildings and structures. The technique has been used regularly to obtain details of construction features and defects. The use of radar techniques to estimate the moisture content and porosity of construction materials poses a severe test of the method. The paper discusses briefly alternative methods of measurement and a number of dielectric models which have been employed as a basis for interpreting measured data.

RÉSUMÉ

Le radar est de plus en plus utilisé dans le cadre des études et évaluations d'une vaste gamme de structures et de bâtiments existants. La technique est régulièrement utilisée pour obtenir des détails sur les caractéristiques et les défauts de construction. L'utilisation d'un radar pour évaluer la teneur en eau et la porosité des matériaux de construction peut représenter un test sévère de la méthode. Cet article aborde brièvement les différentes méthodes de mesures et un nombre de modèles diélectriques qui ont été utilisés pour former la base de l'interprétation des données mesurées.

ZUSAMMENFASSUNG

Tiefenradar kommt bei der Untersuchung und Beurteilung von verschiedenartigen bestehenden Gebäuden und Bauwerken zunehmend zum Einsatz. Das Verfahren wird regelmässig zur Ermittlung von Detailaspekten des Baus und von Fehlern benutzt. Die Bewertung des Feuchtigkeitsgehalts und der Porosität von Baustoffen kann das Radarverfahren schwer auf die Probe stellen. Das Referat behandelt in Kürze alternative Messmethoden und eine Reihe von dielektrischen Modellen, die als Grundlage zur Ausdeutung von Messdaten eingesetzt werden.

1. INTRODUCTION

1.1 The use of subsurface radar has grown considerably in recent years, both as a geophysical tool and for the investigation and assessment of civil engineering structures and buildings. Most commercial radar surveys are carried out using impulse radars. These work by transmitting impulses of electromagnetic energy and receiving energy backscattered (reflected) at discrete interfaces within the medium being surveyed. In general energy is reflected at changes in permittivity, but very thin conductive layers may produce reflections similar to those associated with electrical permittivity variations [1].

1.2 The relative permittivity (ε_r) of dry solids is generally in the range 2 - 8, air has a value of unity and water about 80, in the frequency range of interest. The presence of moisture in a porous media has a large influence upon its effective relative permittivity. For example 'dry' mature concrete $\varepsilon_r \approx 6$, whereas in a saturated mature concrete $\varepsilon_r \approx 12$. This paper discusses briefly alternative methods of measurement and a number of analytical dielectric models which have been employed as a the basis of interpreting measured data.

2. MEASUREMENT TECHNIQUES

2.1 Two different measurement techniques are available employing :

i) air-launched pulses propagated from horn antennas mounted away from the surface being irradiated. This equipment tends to operate at frequencies between about 1 - 3 GHz. Its non-contacting nature allows data to be gathered at high speed and the method has been widely used for pavement thickness evaluations [2].

ii) ground-coupled antennas where the equipment is in contact with the medium being surveyed. Centre operating frequencies range from about 10 MHz to 2 GHz, although frequencies above 500 MHz are most commonly employed on buildings and structures. Ground coupled antennas are sensitive to changes in the permittivity and conductivity of the surface layer of the medium being surveyed. The performance of antennas showing marked variations in some instances.

2.2 Material properties can be evaluated by either reflection or transmission. Air-launched pulses are most commonly used for reflection measurements. As might be expected, such measurements only provide information on the relative permittivity of the material in the surface zone. The transmission technique involves passing a pulse through the media, recording the transit time for a pulse reflected from the rear wall. Accordingly the value of relative permittivity established is an average value for the full depth of member in question. Consider the case of a concrete slab. Millard et al [3] report comparisons of ε_r obtained by reflection and transmission techniques.

Specimen Thickness (mm)	Storage Condition	% Saturation	Estimated ε_r	
			Reflection	Transmission
150	Dry	31	5.8	5.8
400	Dry	41	6.0	8.0
300	Wet	100	10.0	10.2

It will be seen that moisture gradients within porous media can produce erroneous estimates of ε_r as the surface zone is not representative of the body of the media. This can have a significant effect on the estimated propagation velocity and, hence, the estimated thickness of layers. There is a corresponding influence upon any estimates which might be made for the moisture content of the media.

2.3 Another potential source of error is the increase in reflectivity of an interface brought about by the conductivity of the media. In general this is likely to be a small influence at the frequencies employed, unless the effective conductivity at the frequency is large (1 GHz, $\sigma > 0.1$ S/m; 2 GHz, $\sigma > 0.25$ S/m) - refer Figure 1. The DC electrical conductivity of concrete is reported to range from 0.2 S/m for wet concrete to 0.001 S/m for dry concrete. There is little available data concerning the relationship between
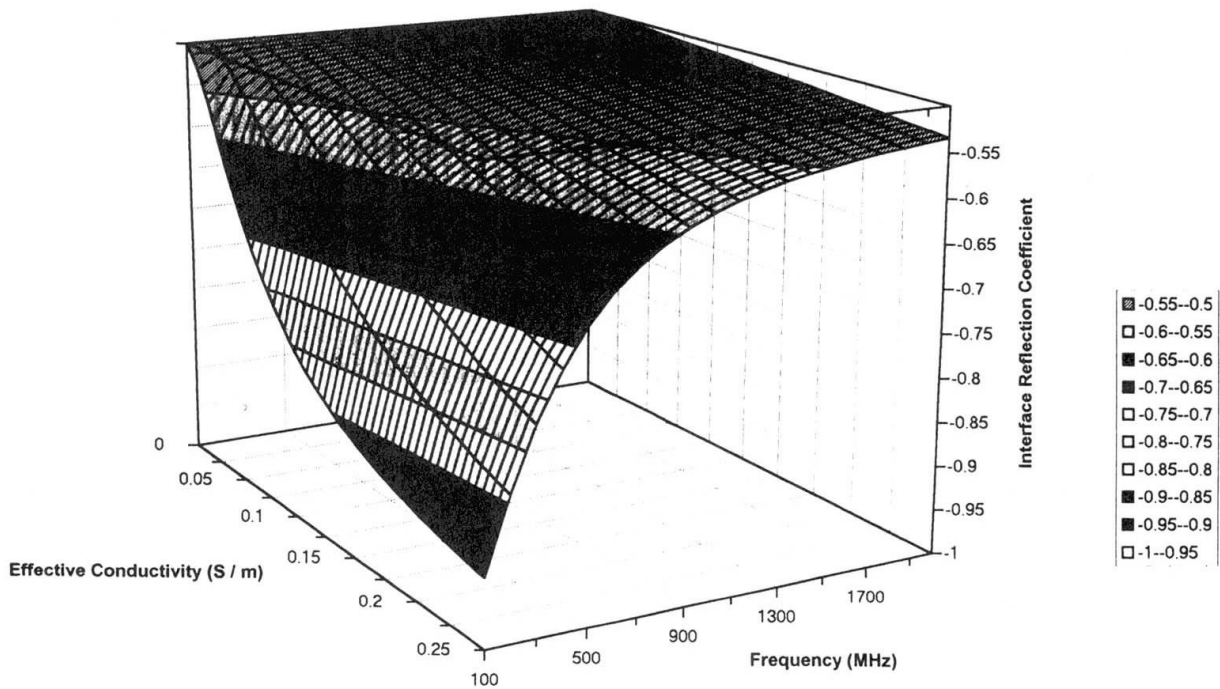
Figure 1 : Interface Reflection Coefficient versus Frequency and Conductivity of Medium 2
(Concrete) for Relative Permittivities, Er1 = 1, Er2 = 9
NB. Conductivity of Medium 1 (Air) = 0

Component Material Properties :
Host (Concrete) Eh = 6 - j0
Inclusion 1 (Saline Water 10 ppt)
Ew = 75 - j57
Inclusion 2 (Air) Ea = 1 - j0
F = 500MHz : T = 20 Deg. C

Figure 2 : Relative Permittivity of Mixture Based on Three Phase Spherical Inclusion Dielectric Model
(after de Loor) Concrete : Water : Air [E* = Em]

DC and effective conductivity at microwave frequencies for construction materials, although effective conductivity is known to increase with frequency.

3. DIELECTRIC MODELS

3.1   The short length of this paper only permits the briefest consideration of the formulation and use of analytical dielectric models. This is a topic of considerable practical interest, the objective being to determine the dielectric properties of a heterogeneous mixture of two or more substances of known permittivities. Factors influencing the average permittivity of a mixture include the permittivities of the individual substances, their volume fractions, spatial distributions and shapes of the constituents and their orientation relative to the electric field vector of the incident el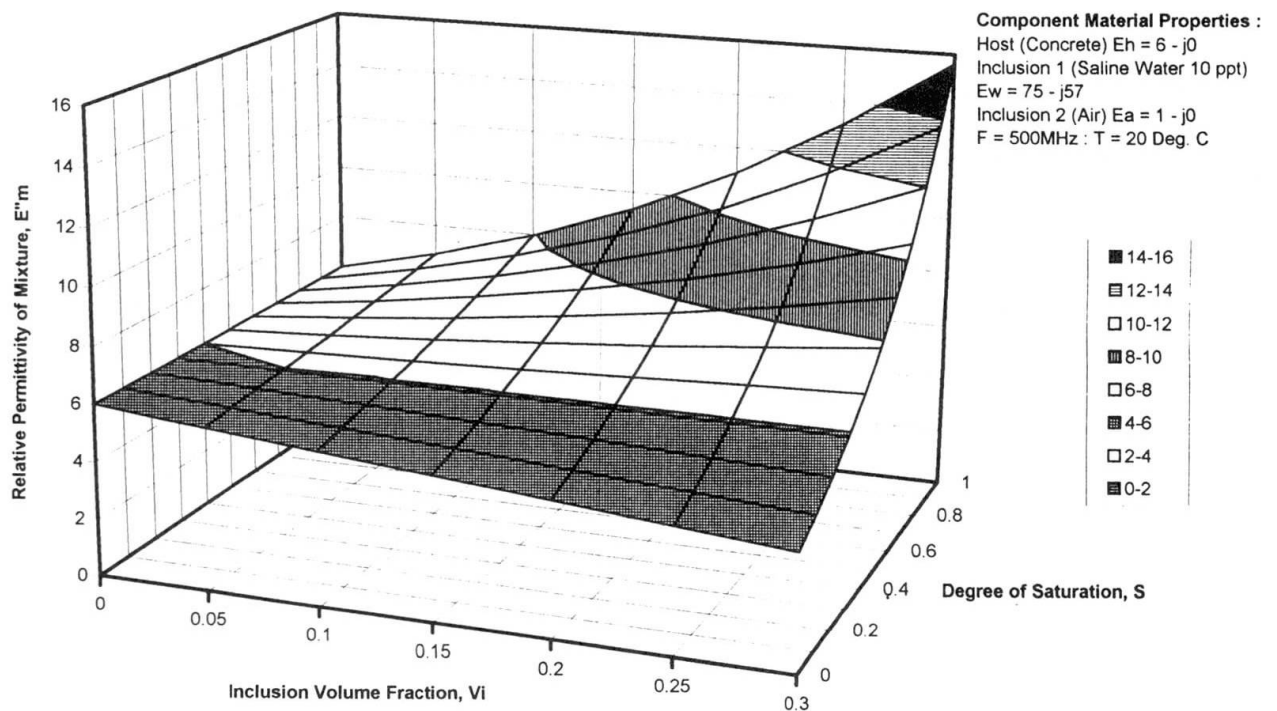ectromagnetic waves. The substance having the highest volume fraction is generally regarded as the host medium, with the other substances being inclusions.

3.2   Many types of dielectric models have been developed and several comprehensive reviews of the topic have been presented in the literature [4,5]. For our current purposes these might be broadly classified into simple volumetric models and geometric dielectric models.

3.3   A volumetric model considers only the volume fraction of the constituents. For a two phase mixture these models generally take the form

$$\varepsilon^{\alpha}_{m} = \varepsilon^{\alpha}_{h} + V_{i} (\varepsilon^{\alpha}_{i} - \varepsilon^{\alpha}_{h}) \tag{E1}$$

where the subscripts m, h and i denote the permittivities of the mixture, host and included material. V_{i} denotes the inclusion volume fraction. A linear mixture model is produced when $\alpha = 1$. When $\alpha = 0.5$ the dielectric model is known as the refractive model (since $\sqrt{\varepsilon}$ = refractive index of medium). Two phase models would arise only in a dry material (construction material solids + air) or a completely saturated material (construction material solids + water). In practice such materials occur rarely and most porous materials are partially saturated (construction material solids + air + water), which requires a three phase model.

3.4   Geometric dielectric models seek to provide a representation of the physical nature of material in question. Such models have a greater range of applicability than simple volumetric models. They are generally much more complicated formulations with attendant difficulties in achieving numerical solutions, particularly when consideration is given to the complex permittivity of mixtures containing water. Figures 2 and 3 illustrate the relationship between relative permittivity and dielectric loss factor of a mixture versus inclusion volume fraction (V_{i}) and the degree of saturation (S). Figures 2 and 3 were derived using Model 2 (see below). The model is based upon spherical inclusions within a concrete host. The difficulty of solving the 'inverse-problem', that is the estimation of the components of the mixture from a determination of relative permittivity and dielectric loss factor, will be appreciated. Such a determination gives a contour line on the surface, further information is needed to achieve a unique solution. Halabe et al [6] have applied similar methods to concrete bridge decks.

3.5   Figure 4 illustrates the relative permittivity of a concrete member estimated by various three phase dielectric models assuming an inclusion volume fraction (V_{i}) of 5%. This would correspond to a poorly compacted concrete. Spherical inclusions have been assumed for geometrical models. For Models 1 and 2 the spherical inclusions are of identical size. Model 5 provides for a continuous size distribution. The dielectric model details are as follows :

Model No.	Model Type
1	Polder-Van Santen-de Loor Formula. $\varepsilon^* = \varepsilon_h$ [7]
2	Polder-Van Santen-de Loor Formula. $\varepsilon^* = \varepsilon_m$ [7]
3	Feng and Sen Formula [8]
4	Linear Volumetric Model [see equation (E1)]
5	Refractive Volumetric Model [see equation (E1)]

Component Material Properties :
Host (Concrete) Eh = 6 - j0
Inclusion 1 (Saline Water 10 ppt)
Ew = 75 - j57
Inclusion 2 (Air) Ea = 1 - j0
F = 500MHz : T = 20 Deg. C
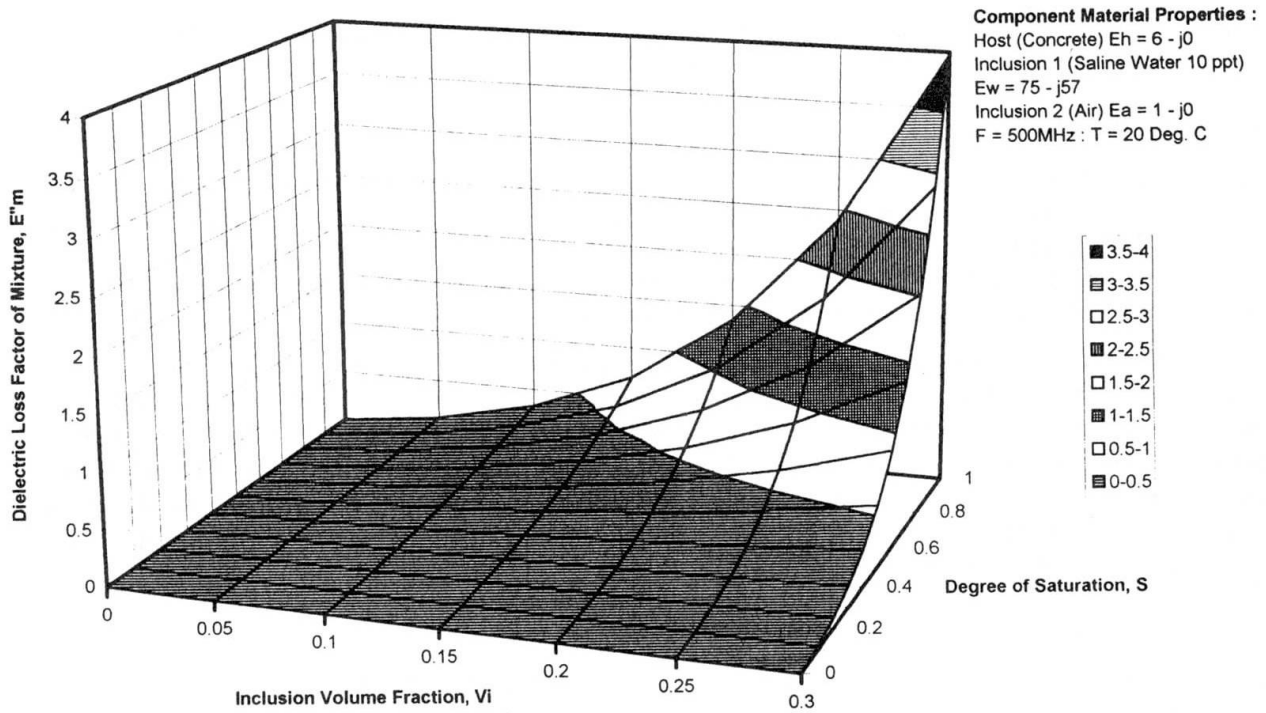
Figure 3 : Dielectric Loss Factor of Mixture Based on Three Phase Spherical Inclusion Dielectric Model
(after de Loor) Concrete : Water : Air [E* = Em]

Component Material Properties :
Host (Concrete) Eh = 6 - j0
Inclusion 1 (Saline Water 10 ppt)
Ew = 75 - j57
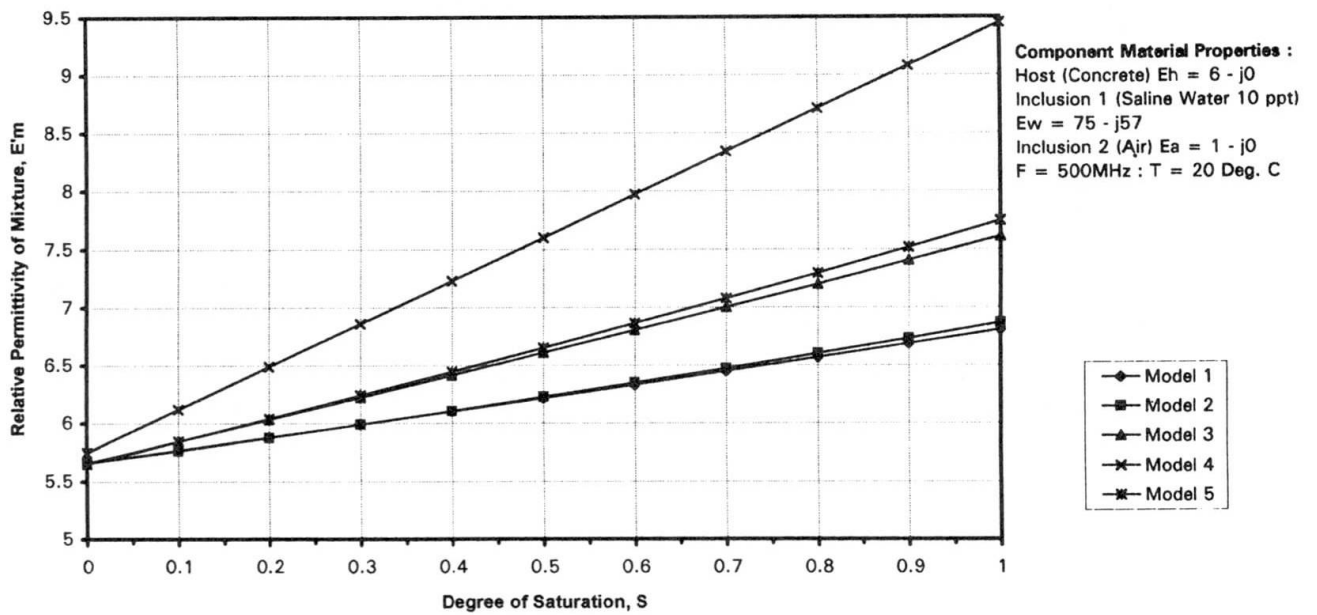Inclusion 2 (Air) Ea = 1 - j0
F = 500MHz : T = 20 Deg. C

Figure 4 : Relative Permittivity of Mixture Based on Various Three Phase Dielectric Models for an
Inclusion Volume Fraction, Vi = 0.05

It is clear that different dielectric models will give substantially different estimates for the degree of saturation, assuming that the inclusion void fraction were known at the measurement location !

4.   CONCLUDING REMARKS

4.1   There is a need to develop dielectric models which match experimental data more closely. The effective medium type theory put forward by Feng and Sen [8] is based on grain shape and does not treat the pore space adequately. This produces computational difficulties. Endres and Knight [9] report different values for ε_r during imbibition and drainage of a porous media. They also note that fine pores have an effect on dielectric behaviour which is out of proportion to their percentage of the total porosity.

4.2   The Building Research Establishment has a programme of research into radar, current interests concern experimental measurements of structural concretes and reinforcing bars, coupled with their analytical modelling. Although it is acknowledged that further studies are required of the nature of porosity with construction materials, there is some concern that the path of ever more complicated dielectric mixture models, which seek to achieve a better representation of the physical reality of the material concerned, may not be particularly rewarding. An alternative approach may be to explore the possibilities offered by artificial neural networks.

REFERENCES

1.   LÁZARO-MANCILLA O and GÓMEZ-TREVINO E, Modelling GPR Reflections from Magnetic Susceptibility and Electrical Conductivity Variations, GPR '94 : Proceedings of the Fifth Int. Conf. on Ground Penetrating Radar, June 12-16 1994, Kitchener, Ontario, Canada, Vol 1, p 79-86.

2.   MASER K R, SCULLION T, RODDIS W M KIM and FERNANDO E, Radar for Pavement Thickness Evaluation, in Nondestructive Testing of Pavements and Backcalculation of Moduli (Second Volume), ASTM STP 1198, 1994.

3.   MILLARD S G, BUNGEY J H and SHAW M, The Assessment of Concrete Quality Using Pulse Radar Reflection and Transmission Techniques, Non-Destructive Testing in Civil Engineering, Proc. Int. Conf. April 14-16 1993, University of Liverpool, Vol 1, p 161-185.

4.   VAN BEEK L K H, Dielectric Behaviour of Heterogeneous Mixtures, Progress in Dielectrics, 1967, 7, p 69-114.

5.   DE LOOR G P, Dielectric Properties of Heterogeneous Mixtures, Applied Science Research, 1964, B11, p 310-320.

6.   HALABE U B, MASER K R and KAUSEL E, Condition Assessment of Reinforced Concrete Structures Using Electromagnetic Waves, Grant No. DAAL 03-87-K005, US Army Research Office.

7.   ULABY F T, MOORE R K and FUNG A K, Microwave Remote Sensing, Vol 3, Appendix E, Artech House Inc, MA, 1986.

8.   FENG S and SEN P N, Geometrical Model of Conductive and Dielectric Properties of Partially Saturated Rocks, J. Appl. Phys., 58 (8), 15 October 1985, p 3236-3243.

9.   ENDRES A L and KNIGHT R, A Theoretical Treatment of the Effect of Microscopic Fluid Distribution on the Dielectric Properties of Partially Saturated Rocks, Geophysical Prospecting, 40, 1992, p 307-324.

X-Ray Diffraction Measurement of Stresses in Post-Tensioning Tendons

Mesure des contraintes par diffraction des rayons X
dans les câbles de précontrainte

Spannungsmessung in vorgespanntem Beton durch Röntgenbewegung

Michael G. CARFAGNO
Structural Engineer
Port Authority of NY & NJ
New York, NY, USA

Faired S. NOORAI
Supervising Struct. Eng.
Port Authority of NY & NJ
New York, NY, USA

Michael E. BRAUSS
R & D Manager
Proto Manufacturing Ltd
Oldcastle, ON, Canada

James A. PINEAULT
Physicist
Proto Manufacturing Ltd
Oldcastle, ON, Canada

SUMMARY

As part of an ongoing inspection and maintenance program for the prestressed, post-tensioned concrete runway extension decks at La Guardia Airport, a state-of-the-art method known as X-ray diffraction was utilized to non-destructively measure stresses in existing post-tensioning tendons. A review of the theory of X-ray diffraction stress measurement is given and a case study of the first known application of X-ray diffraction stress measurement to in-situ post-tensioning tendons as undertaken by the Port Authority at La Guardia Airport is presented.

RÉSUMÉ

Il est ici question d'une méthode relevant de l'état actuel de la technique, connue sous le nom de diffraction des rayons X et destinée à la mesure par essais non destructifs des contraintes dans les câbles de précontrainte; cette méthode fait partie intégrante du programme d'inspection et d'entretien continus des pistes d'aviation exécutées en béton précontraint sur l'aéroport de La Guardia. Les auteurs fournissent un rappel de la théorie de la mesure des contraintes par diffraction des rayons X, ainsi qu'une étude de la première application pratique connue de cette méthode, mise en oeuvre par la "Port Authority" de cet aéroport sur les câbles de précontrainte.

ZUSAMMENFASSUNG

Als Teil des Inspektions- und Wiederherstellungsprogramms für die vor- und nachgespannten Betonflugpisten-Verlängerungsflächen des La Guardia Flugplatzes durch die "Port Authority" wurde eine neuentwickelte Methode der Röntgenbeugung zur Feststellung der Spannungen und Eigenspannung der Verstrebungskabel angewendet. Ein Überblick der Theorie des Messens mit Röntgenbeugung wird gezeigt und eine Fallstudie der ersten praktischen Anwendung der Röntgenbeugung, an Ort und Stelle des La Guardia Flugplatzes wird dargestellt.

1.   BASICS OF THE X-RAY DIFFRACTION STRESS MEASUREMENT TECHNIQUE

The x-ray method does not measure stress directly but does measure strain from which stress values are calculated. The x-ray method takes advantage of the crystalline structure of the material itself by using the interatomic lattice spacing as a strain gage. As a result, thousands of "built in strain gages" within the crystals that comprise the material are available for strain measurement by the x-ray diffraction method. More precisely the surface strain present can be determined by the measurement of the elastic atomic lattice spacing or "d-spacing" as it is commonly called. This lattice spacing, the distance between the planes of atoms, is a function of the material and the stresses present in the material. The x-ray diffraction angle θ for a given x-ray wavelength λ can be used to determine the material "d" spacing by solving Bragg's law:

$$n\lambda = 2d\sin\theta \dotfill \text{Eq. 1}$$

For x-ray diffraction to occur, e.g. constructive wave interference, the path difference traveled by the diffracted beam through the material as compared to a non-diffracted beam, must be equal to $n\lambda$ [1]. The presence of residual stresses in the material produces a shift in the x-ray diffraction peak angular position [2], which is directly measured by the detector. Once the lattice d-spacings are measured for the stressed (d_i) material condition, the atomic lattice strain can be calculated using the known unstressed (d_0) spacing by the following relationship [3]:

$$\text{strain } (\varepsilon) = (d_i - d_0)/d_0 \dotfill \text{Eq. 2}$$

For isotropic materials, strains can be converted to stress values using the equation shown below.

$$\text{stress } (\sigma) = [(d_\psi - d_0)/d_0]\,[E/(1+\nu)][1/\sin^2\psi] \dotfill \text{Eq. 3}$$

where $E/(1+\nu)$ is the x-ray elastic constant, ψ is the angle subtended by the bisector of the incident and diffracted beam and the surface normal, d_ψ is the lattice spacing at a given ψ tilt, and d_0 is the unstressed lattice spacing.

Residual stresses are measured using either of the following two techniques: The first is single exposure technique (SET), whereby a stress measurement is performed using only one tilt angle. This technique gives the user a fast and efficient method to perform a stress measurement and is particularly suited for the need to take many measurements very quickly. The second is the multiple exposure technique (MET), whereby multiple tilts are used in the analysis. This method is more revealing for materials where the relationship between d and $\sin^2\psi$ is not linear, as assumed in equation (3), but takes much longer than the SET [4].

The stress measurements described in this paper were performed using MET with CrKα radiation and the (211) hkl plane.

2.0   APPLICATION TO THE LA GUARDIA AIRPORT RUNWAY EXTENSIONS

2.1   Description of the structure

La Guardia Airport, located in Queens, New York, is bounded by Flushing Bay to the East and Bowery Bay to the West. As a result of the construction of an over-water structure in 1966, Runway 4-22 was extended approximately 610 meters (2,000 feet) northeast into Flushing Bay and Runway 13-31 was extended approximately 305 meters (1,000 feet) west into Bowery Bay to accommodate the first series of Boeing 727 and Convair 880 aircraft.

The structure consists of circular cast-in-place reinforced concrete piles constructed inside a steel shell that support cast-in-place pile caps. Precast, prestressed concrete I-beams span longitudinally (parallel to runways) from pile cap to pile cap. The 40.5 centimeter (16-inch) thick deck slab is supported by the concrete I-beams and is composed of precast, prestressed concrete inverted double tee planks with a cast-in-place concrete topping, which was post-tensioned in both the transverse (perpendicular to runways) and longitudinal directions. Once the deck slab was in place, the I-beams were subsequently post-tensioned to achieve a composite "T" beam in conjunction with the slab. Each runway extension consists of a set of panels approximately 111 meters (365 feet) by 101 meters (330 feet), separated by expansion joints.

The deck slab transverse post-tensioning consists of parabolically draped bundles of 6.35 millimeter (1/4 inch) diameter high strength (f_{pu} = 1,655 MPa = 240 ksi) wires conforming to the BBRV post-tensioning system (Figure 1). The number of 6.35 millimeter (1/4 inch) diameter wires in each tendon varies from 20 to 32 with the spacing of tendons at either 0.75 meter (2'-6") or 1.5 meter (5'-0") intervals, with both parameters, depending on its location, e.g. runway, taxiway or field area. The tendons were initially stressed to $0.7f_{pu}$=1,067 MPa (168 ksi). Depending on the location along the tendon, the theoretical effective stress (after all losses) was initially estimated to range from 986 MPa (143.0 ksi) to 703 MPa (102.0 ksi). After stressing the tendons were grouted.
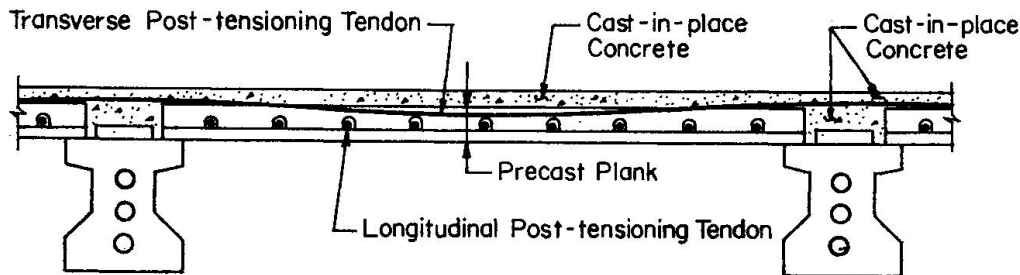

Figure 1:   Typical transverse deck cross section

2.2   Reason for testing

Measuring the actual stress in the transverse, parabolically draped tendons (wires) was undertaken to rule out the possibility of loss of post-tensioning force as a reason for the presence of continuous longitudinal (parallel to runways and I-beams) hairline cracks in the top of the concrete deck in negative moment regions adjacent to the concrete I-beams. X-ray diffraction was the only non-destructive method available that could measure the actual stress without requiring the unloading of a tendon or isolating individual wires, instrumenting them and cutting them free.

2.3   Access and surface preparation

Port Authority personnel core drilled 20.3 centimeter (8 inch) diameter access holes in the runway deck concrete to intersect the transverse (parabolic) tendons (Figure 2) such that it formed a "chord" approximately 4 to 5 centimeters (1.5 to 2 inches) (radial) into the core. Concrete removal was accomplished using a small pneumatic jack hammer just to expose the tendon conduit. The depth of the individual holes ranged from 10 to 25 centimeters (4" to 10") (Figure 2) due to the vertical parabolic drape (Figure 1) of the post-tensioning tendon. Then the conduit (galvanized flexible metal pipe, 0.25 mm =0.01" thick) was peeled back to expose the grouted bundle of 6.35 millimeter (1/4 inch) diameter post-tensioning wires. The grout surrounding the wires was carefully removed by hand with a small chisel. Water and debris were removed from the access hole via compressed air. Surface preparation was not applied to the wire surfaces to be measured.

Site 1 - Adjacent to Taxiway R
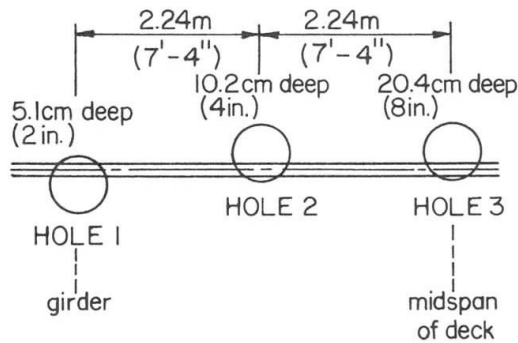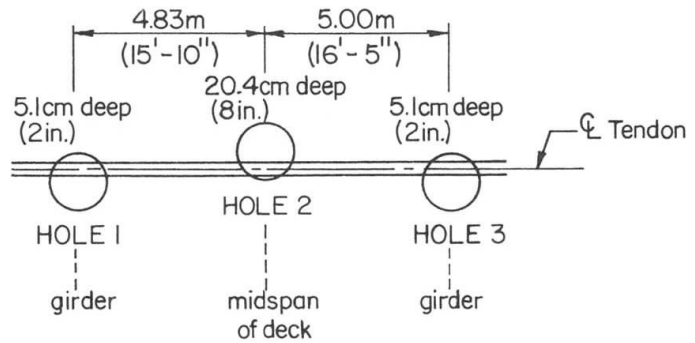
Site 2 - Adjacent to Taxiway P

Figure 2:   Access hole locations and depths,

2.4   Field setup and equipment

An x-ray diffractometer designed specifically for field stress measurements was used to perform measurements. The modular instrument fits inside a van and was powered by a portable generator.
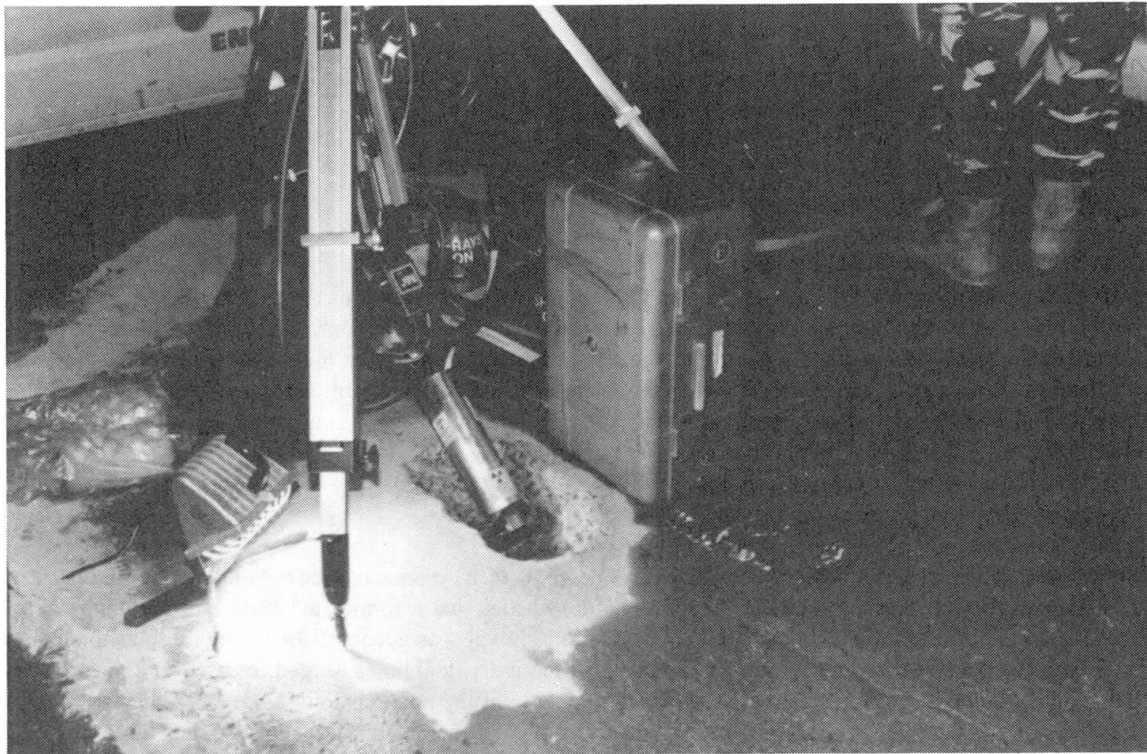

Figure 3:   X-Ray stress measurements being performed adjacent to Taxiway R at La Guardia Airport, New York City. The modular instrument fits inside a van and was powered by a portable generator.

2.5   Stress measurement results

Strain measurements were performed at a total of six locations (two different parabolically draped tendons) on post-tensioned wires embedded in the concrete deck. All measurements were performed at two sites: Site 1 adjacent to Taxiway R and Site 2 was adjacent to Taxiway P. Table 1 gives the resulting calculated stresses at each site and location.

Taxiway	Hole	Wire	Spot	X-Ray Axial Stress (+ = tension) (ksi)	(MPa)	Corrected Axial Stress** (+ = tension) (ksi)	(MPa)	Remarks
P	1	1	1	+12	+83	+17	+184	Wire was struck by jackhammer during concrete removal.
P	1	1	2	+36	+248	+51	+349	
P	1	2	1	+97	+669	+112	+770	
P	1	3	1	+74	+510	+89	+611	
P	3	1	1	+67	+462	+82	+563	
P	3	2*	1	+82	+565	+97	+666	
P	3	3	1	+91	+627	+106	+728	
P	3	4	1	+91	+627	+106	+728	
P	2	1	1	+60	+414	+75	+515	
P	2	2	1	+75	+517	+90	+618	
R	1	1	1	+81	+558	+96	+659	
R	2	1	1	+107	+738	+122	+839	
R	2	1	2	+100	+690	+115	+791	
R	2	2	1	+105	+724	+120	+825	
R	3	1	1	+112	+772	+127	+873	

Table 1: X-Ray stress measurement data
* A section of wire 2 was removed from site 2 after in-situ stress measurements were completed to determine the residual stress and to perform other characterization experiments in the lab.
**Corrected axial stress is measured stress with average estimated residual stress deducted.
The experimental error for each stress measurement ranged from 13.8 to 20.7 MPa (2 to 3 ksi).

2.6   Residual stresses

One 10.2 centimeter (4 inch) section of wire 2 from hole 3, site 2 was carefully removed using bolt cutters. Residual stress measurements were then performed on this section of wire in the lab since the applied stress on the wire due to post-tensioning was removed. All measurements were performed near the center of the specimen so as to avoid areas of localized plastic deformation created during sample removal. The average residual stress measured was -101.4 MPa (-14.7 ksi) (compression). In the case of hole 3 wire 2, the total in-situ stress was measured to be +563.3 MPa (+81.69 ksi) (tension). The average residual stress was found to be -101.4 MPa (-14.7 ksi), hence the applied stress due to the load on this wire can be determined as follows:

Total Stress   = Residual Stress + Applied Stress (due to post-tensioning)
Applied Stress   = Total Stress - Residual Stress
                  = +563.3 MPa - (-101.4 MPa)
                  = +664.7 MPa (+96.4 ksi)

2.7   Calibration procedure

To ensure that the correct elastic constant was used in the calculation of stress using the measured strain data and to determine conclusively the applicability of the wire surface to XRD, a stress/strain relationship was developed. The stress on a 10.2 centimeter (4-inch) section of wire taken from hole 3, site 2 was measured under an incremental uniaxial tensile loading regime. The load was monitored using a load cell and by a strain gage during x-ray data collection.

The generally accepted values of Young's Modulus (E) and Poisson's Ratio (v) for steel are 200,000 MPa (29,000 ksi) and 0.29 respectively. The close agreement of the experimentally determined Young's Modulus of 196,294 MPa (28,469 ksi) ± 2096 MPa (304 ksi) with the generally accepted value gives the strain gage data credibility and demonstrated the linearity of this relationship. The data collected at zero strain and zero load was ignored since there was some slack in the fixture, which caused low readings to be anomalous.

A plot of x-ray stress vs. stress calculated using strain gage strain readings was created. This data was used to determine the experimental value for E/(1+v). The x-ray stress was calculated using the generally accepted values of E and v. When the stress under the loading regime was plotted against the stress calculated using the strain gage data, we would expect a slope equal to 1 in the case where the generally accepted value for E/(1+v) was the correct one for the particular alloy being tested. This is rarely the case, thus an experimental x-ray value for E/(1+v) must be determined.

$$
\begin{aligned}
K_{x\text{-}ray} \quad &= K_{mechanical} / 0.868033 \\
&= 155,006 \text{ MPa} / 0.868033 \\
&= 178,572 \text{ MPa} (25,899 \text{ ksi})
\end{aligned}
$$
and the ratio $1/0.868033 = 1.15203$

With this new x-ray elastic constant, the slope of the x-ray stress vs. strain gage stress plot will be equal to 1. Hence, all stress measurement values obtained at LaGuardia were adjusted by this factor.

2.8   Conclusions

At site 1 adjacent to Taxiway R, total stress measurements ranged from +560.6 MPa to +774.3 MPa (+81.3 ksi to +112.3 ksi) (tensile). At site 2 adjacent to Taxiway P total stress measurements ranged from 460.6 MPa to 669.7 MPa (+66.8 ksi to +97.13 ksi) (tensile). One reason for the range in readings is that the stress in the tendon varies with the location along the parabolically draped tendon due to friction losses that occurred while stressing the tendon. It should be noted that the x-ray diffraction method measures the stress only at the surface of the sample. Assuming an average compressive residual stress of 101.4 MPa (14.7 ksi) for all wires, to arrive at a number for the actual applied tensile stress in the wire due to post-tensioning, the 101.4 MPa (14.7 ksi) must be added to the observed measurements. After making this adjustment, the measured tensile stresses were found to be in rough agreement (within 20%) with the calculated estimate of stress in the tendon after losses. One explanation for the compressive residual stress is that the wires were drawn through a die that induced residual stresses. Because the measurements could only be made on the outer layer of wires in the bundle it is not known if the outer wire stress is representative of the average wire stress in the bundle which is the basis for the theoretical computation.

The x-ray diffraction method of measuring stresses proved to be a relatively simple and efficient technique to non-destructively measure stresses in post-tensioning steel wires in an existing concrete member. It would be of value if the technique could be tested in a laboratory setting and readings taken on interior and exterior wires under post-tensioning forces as well as, correlation being made directly with instrumented wire tensile stresses.

REFERENCES

[1] I.C. NOYAN, J.B. COHEN, Residual Stress Measurement by Diffraction and Interpretation. Springer-Verlang, 1987.

[2] B.D. CULLITY, Elements of X-Ray Diffraction, Addison-Wesley Publishing Co., 1978.

[3] M.E. HILLEY ET AL, Residual Stress by X-Ray Diffraction - SAE J784a, Society of Automotive Engineers, Inc., 1971.

[4] H.P. KLUG, L.E. ALEXANDER, X-Ray Diffraction Procedures, 2nd Edition, Wiley-Interscience, 1974.

Non-Destructive Inspection System for Welded Portions of the Honshu-Shikoku Bridges

Système de contrôle non-destructif des parties soudées dans les Ponts Honshu-Shikoku

Zerstörungsfreie Prüfung von Schweissverbindungen in den Honshu-Shikoku-Brücken

Chikara MIYASHITA
Dir., Maintenance Dept
Honshu-Shikoku Bridge Auth.
Tokyo, Japan

Kenzou BABA
Dir. 2nd Maintenance Dept
Honshu-Shikoku Bridge Auth.
Tokyo, Japan

Hiroaki HOASHI
Dep. Mgr, Maintenance Dept
Honshu-Shikoku Bridge Auth.
Tokyo, Japan

SUMMARY

The Kojima-Sakaide route of the Honshu-Shikoku Bridges consists of the world's first large-scale combination of highway and railway bridges. Design and fabrication were conducted with consideration for fatigue based surveys in truss members subjected to railway loads. This report outlines the non-destructive inspection system developed for prompt detection of any fatigue cracks that may be generated in the bridge during usage, and also for evaluation of the cracks based on fatigue analysis.

RÉSUMÉ

L'itinéraire Kojima-Sakaide des ponts entre Honshu et Shikoku est la première véritable grande liaison au monde combinant le rail et la route. Le comportement à la fatigue des treillis soumis à la charge des trains a été prise en due considération tant au stade de la conception qu'au stade de la construction. La Honshu-Shikoku Bridge Authority a mis au point un système de contrôle non-destructif des soudures visant à déceler le plus tôt possible les fissures de fatigue et à évaluer leur évolution par une analyse de la fatigue.

ZUSAMMENFASSUNG

Der Kojima-Sakaide-Abschnitt des Honshu-Shikoku-Brückensystems besteht aus der ersten grossen Kombination aus Strassen- und Bahnbrücken der Welt. Überlegungen zur Ermüdung von Fachwerkstäben unter Eisenbahnlast werden in Planung und Ausführung berücksichtigt. Es wurde ein Verfahren zur zerstörungsfreien Prüfung von Schweissarbeiten entwickelt, um eine rasche Erkennung von Ermüdungsrissen in der Brücke, eine Auswertung von Rissen basierend auf Ermüdungsanalyse sowie geeignete Wartungs- und Instandsetzungsarbeiten zu ermöglichen.

1. INTRODUCTION

The Kojima-Sakaide route, often called the Seto Ohashi Bridges, of the Honshu-Shikoku Bridges, consists of the world's first large-scale combination of highway and railway bridges. Design and fabrication were conducted with consideration for fatigue based on years of surveys of fatigue in truss members subject to railway loads. A record of inspections during the fabrication process has been kept.

Since the Seto Ohashi Bridge was opened for service in April 1988, advanced maintenance for its important role has been required. The maintenance of fatigue cracking in welded portions is especially important to ensure the soundness of the bridge.

This report outlines the "Non-destructive Inspection System for Welding on the Seto Ohashi Bridges," which was developed for prompt detection through non-destructive inspection of any fatigue cracks that may be generated in the bridge during usage, and also for the evaluation of the cracks based on fatigue analysis. The report covers not only considerations for fatigue in the design and fabrication stages, but follow up and evaluation of fatigue strength during usage.

2. DESIGN, FABRICATION, AND INSPECTION OF TRUSS MEMBERS BASED ON EVALUATION OF FATIGUE

The fatigue design of the Honshu-Shikoku Bridge is based on how fatigue cracks advance. By preventing fatigue cracks from penetrating the steel plate, during the durable years (100 years) of a bridge established in the design, serious damage to it can be avoided. When fabricating members, fatigue of the main chord members is given primary consideration. With corner welds on the main chord members, for example, design and fabrication is based on the following ideas:

① Fatigue cracks are generated from welding failure in the blow holes of the root portion.

② Fatigue cracks are generated in the early stages of repeated stress and fatigue life is almost the same as crack advancement life.

③ The number of repetitions of fatigue cracks advancing 80% the distance from the root to the surface of the plate is considered to be a measure of the end of fatigue life.

④ Welding failure of blow holes that generate fatigue cracks cannot be completely avoided, so allowable values of initial failure in fabrication should be set and places where failure exceeds these values should be repaired.

As Table 1 shows, based on these ideas, in fabricating members of thermal refined high strength steel, members are classified according to the ratio of their working stress range and their allowable stress range, and allowable dimensions of failure are determined for each member. For detection of failure in corner welds, ultrasonic flaw examinations, in which blow holes as small as about 1 mm can be detected, are done. In fabrications in use, all failures exceeding allowable values are repaired and those within allowable values are recorded for future maintenance management servicing.

Member class	Working stress range (σ_r) / allowable stress range (σ_{fa})	Allowable dimensions	Notes
Special A	$0.7 \leq \dfrac{\sigma_r}{\sigma_{fa}}$	$W \leq 1.5\text{mm}$ $H \leq 4\text{mm}$	
A	$0.5 \leq \dfrac{\sigma_r}{\sigma_{fa}} < 0.7$	$W \leq 3\text{mm}$ $H \leq 6\text{mm}$	
B	$\dfrac{\sigma_r}{\sigma_{fa}} < 0.5$	$W \leq 3\text{mm}$ $H \leq 6\text{mm}$	

Table 1 Classification of inspection standards of members using thermal refined high strength steel (corner welds)

Compared to inspections done during fabrication at the factory, however, the following problems exist with non-destructive inspections of actual bridges:

① Crack locations are difficult to determine.

② Means of approaching members closer are inadequate.

③ Inspections are done from all angles.

④ Inspections are done from above the coating.

To deal with these problems, a committee for examining the non-destructive inspection system being used was established and investigations related to the above problems were done over a period of four years as the bridge was built.

3. EXAMINATIONS ON ACTUAL BRIDGES

3.1 Confirmation of automatic ultrasonic flaw detection technology

3.1.1 Improvement of ultrasonic flaw detectors

Equipment was developed featuring the improvements listed below and no performance sacrifices over equipment used in inspections during fabrication.

① As Figure 1 shows the main unit has the following components: ultrasonic flaw detector, computer, controller, and plotter.

② The probe scanner is small and light, and the device has a new structure that enables inspections to be done above and to the sides.

③ Data is stored on floppy disks so it can be reexamined, which heightens the accuracy of flaw detection evaluation.

④ In addition to corner joints, the automatic flaw detection function can now be used on butt joints and T-joints.

Figure 2 shows the probe arrangement for inspecting corner joints with the equipment. As with the equipment used for doing inspections during fabrication, penetration depth is measured with the point focusing vertical probe P, and failure inspections are done with the point focusing beveled probes (reflection angle of 45°) F-AF and F-AB and the point focusing vertical probe F-N. The results are output as shown in Figure 3. Results of inspection with the three probes for flaw inspection are shown in columns FLAW-N, FLAW-AF, and FLAW-AB. LEVEL shows the peak echo values of each scan line, and PLAN VIEW shows the shapes of penetration lines and flaws (marked in white) as observed from the surface of the detected flaw.
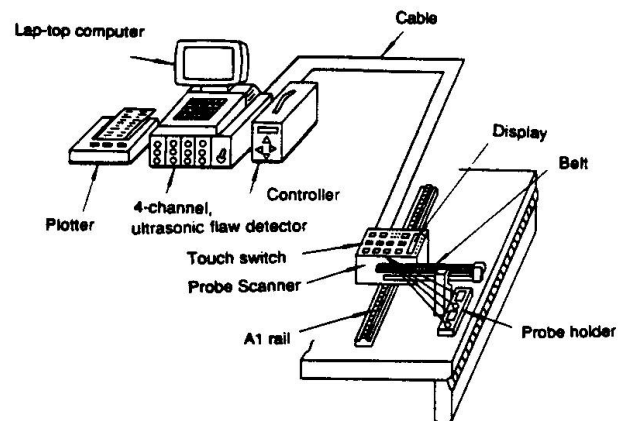

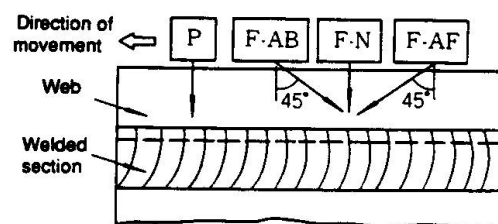Fig. 1 Configuration of the small, automatic, ultrasonic flaw detector

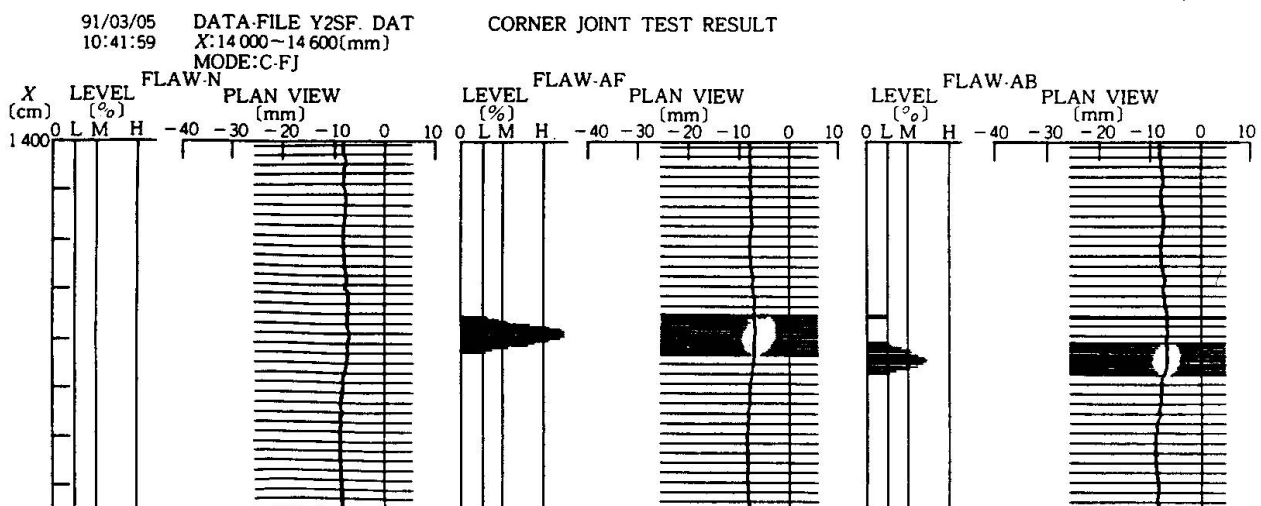Fig. 2 Probe arrangement for flow inspection of corner joints

Fig. 3 Example of results of an inspection conducted with the equipment developed

3.1.2 Confirmation of the applicability of the equipment to field inspections

Field flaw detection tests were done on the Kitabisan Seto Ohashi Bridge to examine the applicability of the equipment developed. The primary objects of the tests were as follows:
  1) Ability to reach inspection points
  2) Effects of equipment positioning
  3) Effects of coating

Automatic ultrasonic flaw detection was done during fabrication and before coating; each member of bridges in use was coated to a thickness of 255 μm. Therefore, places where blow holes of less than the allowable value remained were field inspected and the effects of coating on flaw detection was examined. The results are shown in Table 2. Surfaces of detected flaws were coated to a thickness of 288-307 μm, but the results were the same as in tests conducted during fabrication. It was confirmed that there were no problems in detecting flaws through the coating.

Field tests showed that, by using the equipment developed, the same inspections done during fabrication can be done on bridges in use, inspection data collected during fabrication can be followed up on in field inspections, and new data can be accumulated.

	Result of inspection during fabrication		Result of field inspection		
Flaw No.	Estimated flaw dimensions		Coating thickness	Estimated flaw dimensions (mm)	
	Width	Height	(μm)	Width	Height
79	0.8	1.5	279-288	0.7	1.6
80	0.8	1.4	295-307	0.8	1.2

Note) The same probes and sensitive standard test pieces were used to set sensitivities at the same levels.

Table 2 Comparison of inspection during fabrication and field inspection

3.1.3 Examination of the method for measuring the frequency of fatigue stress

To rationally determine inspection frequency and the need for repairs by analyzing fatigue life with a non-destructive inspection system, it is important to accurately estimate the degree and frequency of stress on evaluation points. Therefore, to predict the frequency of stress on actual bridges by using data collected in stress analysis in the design phase, the frequency of fatigue stress on each member of the Kitabisan Seto Ohashi Bridge was measured and analyzed.

4. CONSTRUCTION OF A NON-DESTRUCTIVE INSPECTION SYSTEM

Based on the results of the above examination and measurements from field tests, a non-destructive inspection system was designed and an interactive system featuring personal computers with user-friendly menus was developed.

4.1 System functions

Figure 4 is a flow chart of the system, which has the following five primary functions:

  1) Retrieving and updating flaw data
     All data on flaws detected through non-destructive inspection during fabrication which are less than the allowable value are input into a table. Data can be retrieved, and new data obtained during inspections can be input.
  2) Display of the distribution of flaw data
     Data on blow hole size, which constitutes most of the detected failure data, were classified into classes A to D. The distribution of the frequency of flaws on each member is displayed as shown in Figure 5. In addition, for members with Class A or B flaws, data detailing the location and dimensions of each flaw are displayed as shown in Figure 6.
  3) Display of fatigue design data
     The class of each member according to the required quality and fatigue design stress range are displayed.
  4) Fatigue analysis
     Fatigue crack advancement analysis using flaw data collected through non-destructive inspection and fatigue strength analysis of welded joints where the generation of fatigue cracks is a concern were done to rationally determine inspection frequency and the need for repairs.
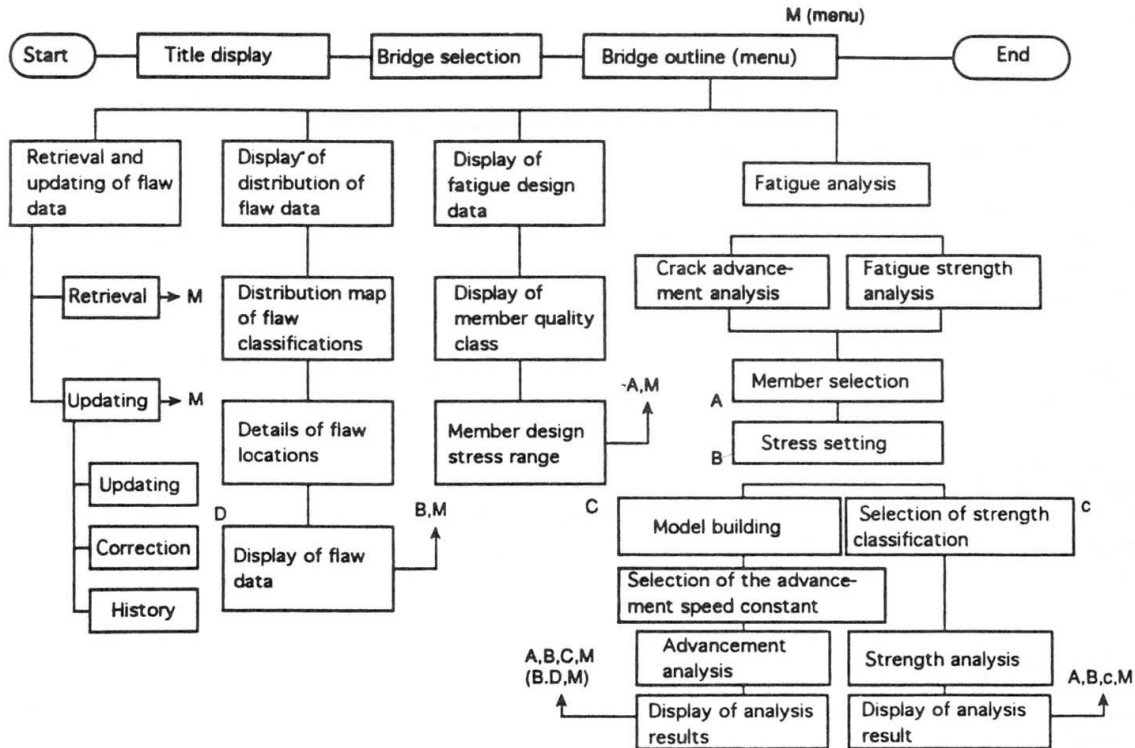
Fig. 4 System flow chart

The contents of the crack advancement analysis are shown below. In the equations of fatigue crack advancement speed, numerical integration is repeated from the initial crack dimensions a_i to the crack dimension limit a_f.

$$da/dN = C(\Delta K^n - \Delta K_{th}{}^n) \quad \ldots\ldots\ldots (1)$$

$$da_i = C(\Delta K^n - \Delta K_{th}) \cdot dN_i$$

where, da/dN: fatigue crack advancement speed

ΔK: range of the stress expansion coefficient

C, n: constant

ΔK_{th}: range of lower limit of stress expansion coefficient

With this system, 11 analytical models, including a root blow hole model, are used in accordance with the characteristics of the members of the Honshu-Shikoku Bridges. When selecting which evaluation model to use, the stress expansion coefficient ΔK in the equation (1) is automatically determined. ΔK is expressed below.

$$\Delta K = \Delta\sigma\sqrt{\pi a} \cdot F$$

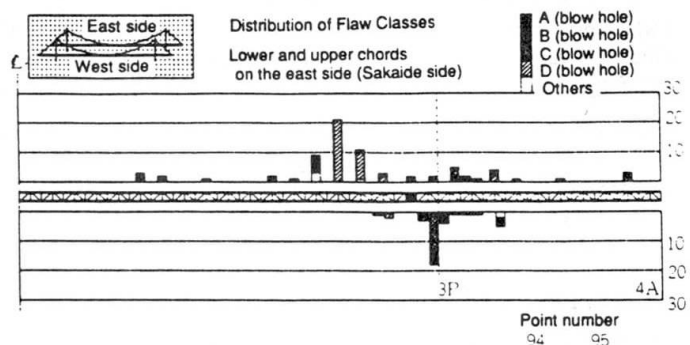where, $\Delta\sigma$: stress range

a: crack dimensions

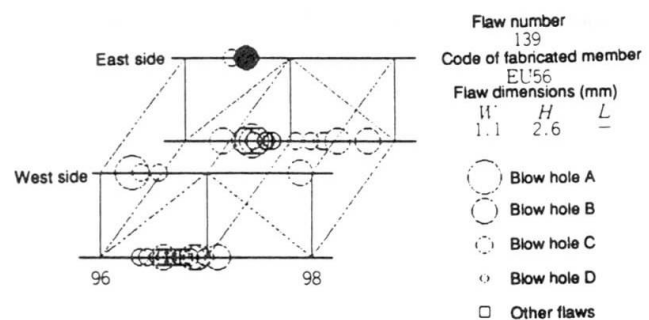Fig. 5 Distribution of flaw class

Fig. 6 Details of flaw cocations

F: correction factor for concentrated stress on and crack shapes of joints

The first step in the analysis is to input the initial flaw dimensions a_i Then, based on the examination results derived with the method in Section 3.1.3 for predicting fatigue stress frequency, fatigue loads preset for each member are set. (Since the secular change of traffic load conditions can be input in the form of a coefficient, analysis incorporating changes in traffic volume after the bridge is in use and predictions can be conducted.) When crack advancement speed data C, n, and ΔK_{th} are set from data obtained by the Honshu-Shikoku Bridge Authority, the system automatically analyzes crack advancement and the results are displayed in the form of a crack dimension curve and a crack shape diagram, as shown in Figure 7. Fatigue strength analysis can also be done with the system.
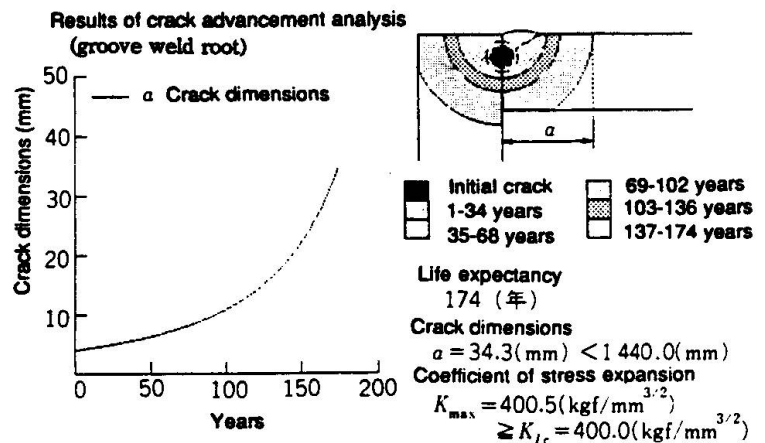
Results of crack advancement analysis (groove weld root)

Initial crack
1-34 years
35-68 years
69-102 years
103-136 years
137-174 years

Life expectancy
174 (年)

Crack dimensions
$a = 34.3(mm) < 1 440.0(mm)$
Coefficient of stress expansion
$K_{max} = 400.5(kgf/mm^{3/2})$
$\geq K_{Ic} = 400.0(kgf/mm^{3/2})$

Fig. 7 Example of results of crack advancement analysis

4.2 Configuration of system hardware

The system has a 32-bit IBM personal computer (40MB hard disk, built-in 2-drive floppy disk, and an additional 6MB of extended memory) and a color printer.

5. CONCLUSION

Based on studies of fatigue on the Honshu-Shikoku Bridge and tests on actual bridges for verification of conditions for systematizing technologies, a comprehensive non-destructive inspection system was developed. The system enables the following: retrieval and distribution display of flaw data obtained in ultrasonic flaw inspections of the Kitabisan Seto Ohashi Bridge; and, with consideration for stress frequency and member characteristics, fatigue crack advancement analysis and fatigue strength analysis.

There are many cases in which accurate surveys and analyses must be urgently done to evaluate the soundness of a large bridge. However, with this system, these types of survey and analysis can be performed in daily inspections. Therefore, this system is very useful for proper maintenance management of the Seto Ohashi Bridges. In the future, we are planning to extend use of the system to other bridges.

6. REFERENCES

1) Bridge and Offshore Engineering Association (commissioned by the Honshu-Shikoku Bridge Authority): Committee for Examining the Fabrication of Members of the Honshu-Shikoku Bridge (Chairman, Toshie Okumura)

2) Japan Society of Civil Engineering (commissioned by the Honshu-Shikoku Bridge Authority): Subcommittee for the Study of Steel Superstructures, Fatigue Examination Committee (Examination Committee Chairman, Toshio Nishimura)

3) Bridge and Offshore Engineering Association (commissioned by the Honshu-Shikoku Bridge Authority): Examination Report on Application of the Non-destructive Inspection System to Bridges in Use (1988.3) (Chairman, Jiro Tajima)

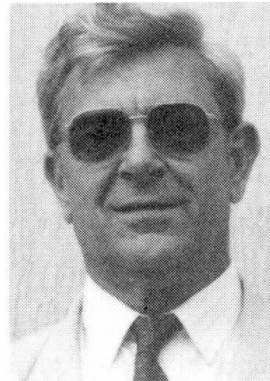4) Japan Steel Structure Corporation: Fatigue Design Guidelines (plans), JSSC Report No. 14 (1989)

Surveillance Programme for Stay Cables
Programme de surveillance des haubans
Überwachungsprogramm von Schrägseilen

Jean-Phillipe FUZIER
Scientific Director
Freyssinet International
Vélizy, France

Roger LACROIX
Consulting Engineer
Paris, France

SUMMARY

It is not unusual for structures today to be required to have 120 years lifespans or more. This is not only an economical requirement of the developed countries, but also reflects the desire to build better quality structures. The way to meet this demand of modern construction is to develop maintenance and monitoring systems. Structures must provide all facilities to ease maintenance operations. This paper proposes a tentative surveillance programme which could be set up for stay cables through the example of the Normandy Bridge. The frequency of inspections, their nature and their contents are examined.

RÉSUMÉ

Les autorités publiques demandent aujourd'hui des durées de vie de 120 ans et plus. Au-delà de la nécessité économique des pays développés, il y a le désir de construire mieux et de meilleure qualité. Une réponse à cette exigence des constructions modernes est le développement des programmes de surveillance et de maintenance. Cet article envisage le cas des ponts à haubans, des haubans eux-mêmes, à travers l'exemple du pont de Normandie.

ZUSAMMENFASSUNG

Heutzutage verlangen die Behörden Lebensdauern von 120 Jahren oder mehr. Dies ist nicht erstaunlich; jenseits von den wirtschaftlichen Bedürfnissen der entwickelten Länder äussert sich tatsächlich der Wunsch, besser und mit einer zunehmender Qualität zu bauen. Die Entwicklung der Überwachungs -und Wartungsprogramme antwortet auf diese Forderung an die modernen Bauwerke. Dieser Artikel spricht von Schrägseilbrücken und Schrägseilen insbesondere am Beispiel der Normandie-Brücke.

1. INTRODUCTION

The need to maintain the existing infrastructures, of which bridges comprise an important part, induced many developed countries to conduct a survey of the bridge maintenance problem from both technical and economical point of view. It is of common understanding in Europe that the maintenance needs are given in terms of percentage of total bridge renewal value. Figures vary between 0.5 to 1.5% [1]. A simplified approach to this problem would lead to a lifespan of 170 years if the renewal percentage is 0.6 and 500 years if the percentage is only 0.2!. These figures indicate only one reason for having long lifespan. Since there are no products suppliers able to give a 100 or 120 years guarantee for their supply, we understand that monitoring and maintenance are a real need.

Large structures, like cable stayed bridges, which span estuaries or large rivers, have to be monitored and maintened.

2. CABLE STAYED BRIDGE SURVEILLANCE

2.1 General

The main reasons for maintenance of a cable stayed bridge are [2] [3] :

> - to control the functional requirements and provide assurance that the structure is safe and fit for its designated use.

> - to identify actual and potential sources of trouble and misuse at the earliest possible stage.

> - to monitor the influence of the environment.

2.2 Monitoring of the Normandie bridge

We are referring hereafter to the permanent surveillance of the bridge during operations. This does not cover the measures which were carried out during the various construction stages and during the static and dynamic testing.

Measurement will be automatically recorded and stored in a computer centre close to the toll building. The following data will be measured and monitored:

> - Wind speed at mid span (for traffic control).
> - Temperature at 7 points of a steel deck cross section.
> - Temperature at 7 points of a concrete deck cross section.
> - Temperature at 8 points of a pylon cross section.
> - Stress in the stay cables : 4 stay cables will be equipped.
> - Temperature on one stay cable.
> - Stresses in the steel deck at mid span (10 extensometers)
> - Deflections and accelerations at pylon heads.
> - Various accelerometers for vibration surveillance (pylon, deck and stay cables)
> - Stresses in the steel deck at stay cable anchorage locations.

- Movements of expansion joints.
- Air humidity content in the steel box girder.
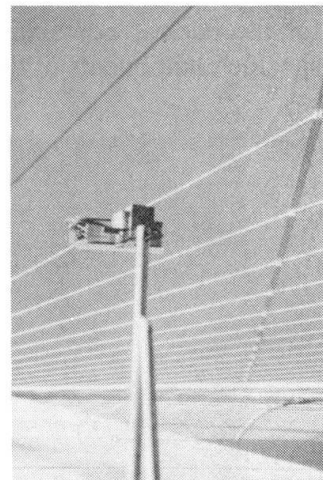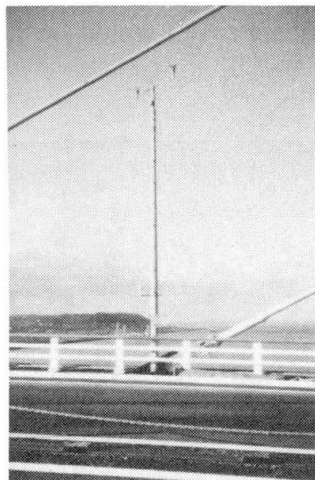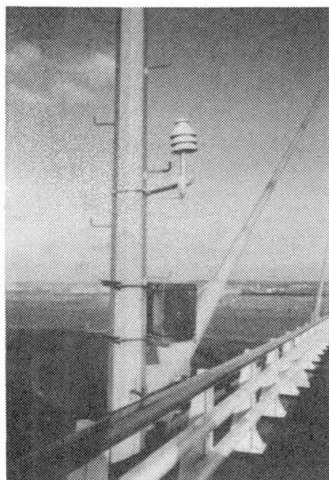
3. STAY CABLE MONITORING AND SURVEILLANCE

3.1 General

Instrumentation and permanent observation of the behaviour of large dams or nuclear plant facilities is common practice today. The same process used by American engineers from the U.S. Nuclear Regulatory Commission for the prestressing of the containment vessels is proposed to be used for the stay cables. This process would imply that arrangements be made during the construction study, so that expert appraisals can be carried out without any interruption to the structure's functioning.

The surveyed elements must be in easily dissociable simple units, so as to leave no doubt about the level of their characteristics during the surveillance, and therefore, the condition of the structure. The Freyssinet stay cable, with its individually protected strands, has been designed to be suitable for surveillance.

3.2 The Freyssinnet stay cable concept

This is a perfectly reversible assembly. Let us just recall that it can be installed and dismantled using only light equipment, with no interruption to traffic, and that no surveillance operation interferes with the bridge's serviceability.

The surveillance is carried out on the three essential parts of a stay cable : the actual cable, the anchorage areas, the transition areas :

- The cable, composed of a bundle of parallel strands, with no rigid link between them, remains accessible to investigation on any strand : weighing, slackening, removal for detailed inspection.

- The anchorage areas are subjected to surveillance operations including external visual inspection, inspection of the anchorage, analysis of the wax, weighing of the stay cable, inspection of the adjustment threads.

- The transition areas are also subjected to a visual inspection prior to and after dismantling, and to an expert appraisal of certain materials (neoprene, mastic compound, plastic,....).

Basically the frequency of visits, their nature and the contents of the surveillance report must be defined. Right from the time of test-loading the bridge, surveillance operations for 1 year, 3 years, and 5 years later and thereafter every 5 years for the complete life of the bridge could be specified, as for the nuclear containment. A better approach would be to adapt the recurrence period to each specific components of the stay cable.
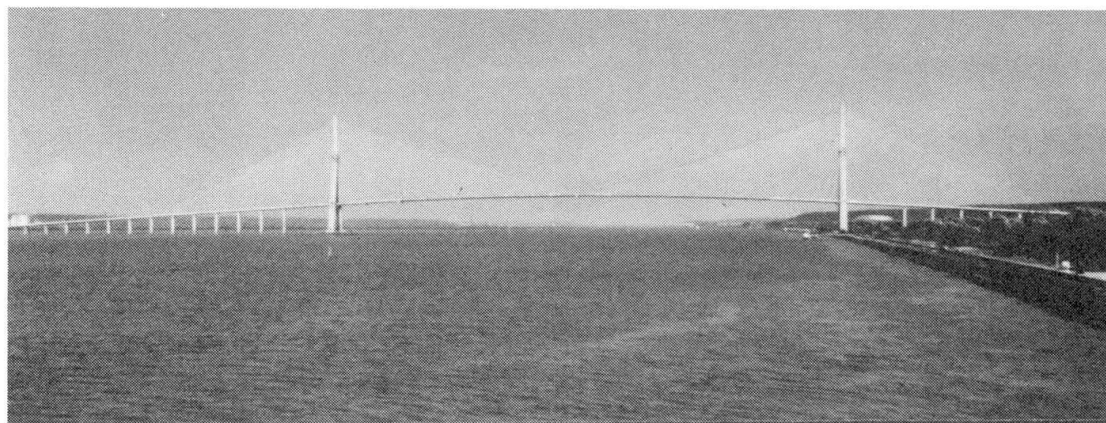

3.3 Proposed surveillance programme for Normandie bridge.

The following programme has been proposed :

MAINTENANCE PROGRAMME	FREQUENCY MONTH	QUANTITY %
1. DECK		
Guide pipe on steel deck	12	25
Deviator-guide on steel deck	60	25
Anti-vandalisme pipe	12	25
Lighting system	12	50
Damper	24	100
Injection caps on steel deck	12	25
Stay cable anchorage on steel deck	24	25
Anchorage of dampening ropes	24	25
Injection caps on concrete deck	30	25
Stay cable anchorage on concrete deck	36	25
2. PYLON		
Injection cap, adjusting nut	12	50
Stay cable anchorage	24	25
Tensioning systeme	12	100
External face of the pylone	48	100
Dampening ropes	12	25

SPECIAL PROCEDURES

Retensioning or detensioning of a stay cable
Partial or total replacement of a stay cable
Replacement of a dampening rope
Replacement of aerodynamic sheath component
Replacement of lighting collar
Replacement of anti-vandalisme pipe
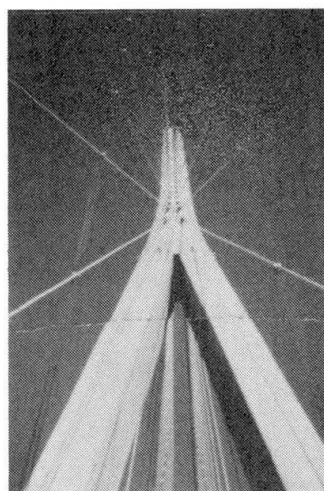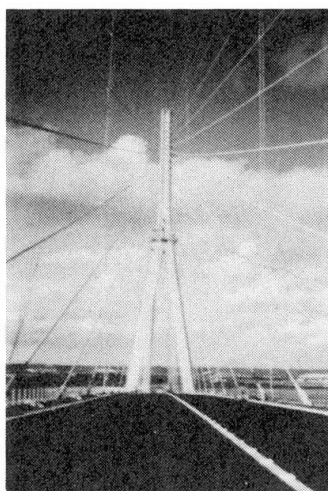
"Normandie bridge dampening ropes"

4. CONCLUSION

To conclude this paper, let us remember the new aspect which we wish to confer on surveillance, that is to adapt in relation to structural maintenance, a new state of mind, a new attitude, with the object of obtaining from owners an undertaking to include surveillance right from the origin of the project and to consider it as forming part of their investment and not just a badly defined maintenance cost which depends upon the manner in which the structure ages.

Surveillance, seen from this angle, is an intentional step which aims at preventing disorders and results in avoiding large repair works which cause interruption of traffic, particularly on large bridges. Its costs should be considered both in terms of service and good management with respect to public funds or in the interest of shareholders. But we should remember that no matter how perfect the project may be, the quality of behaviour in service of the structure, depends essentially on the treatment of finishing details, both in the design stage and during construction. Satisfactory durability depends on this, and it is illusive to count for inspection and surveillance afterwards if the construction has not been, first of all, carried out properly.

REFERENCES

[1]   OECD - Durability of Concrete Road Bridges, 1989.

[2]   FIP - Guide Inspection and Maintenance of Reinforced and Prestressed Concrete Structures.

[3]   M. Wieland "Instrumentation aspects of Cable stayed bridge Bangkok 18-20 November 1987.

[4]   K. Ostenfeld - H. Langsoe
" Full scale measurement and monitoring of major cable stayed bridge"
Bangkok 18-20 November 1987.

Monitoring System for a Large Cable-Stayed Bridge in a Wind and Seismic Area

Système de surveillance d'un grand pont dans une zone de vents et de séismes

Ueberwachungssystem für eine grosse Brücke in einer Gegend mit Taifunen und Erdbeben

Helmut WENZEL
Dr-Ing.
Vienna Consulting Eng.
Vienna, Austria

Helmut Wenze is member of WC 5 of IABSE. He earned a Ph.D. in Bridge Construction from the University of Vienna in 1978. He is the Managing Director of VCE, with offices in Vienna, Taiwan and Korea. Dr. Wenzel also teaches Bridge Design and Construction at the University of Vienna.

SUMMARY

To understand the behaviour of a major bridge under extreme loading conditions, an innovative Monitoring System was designed to be implemented in the Kao Ping Hsi Bridge in Taiwan. This innovative bridge is located in an area with frequent typhoons and a considerable number of earthquakes per year. The aim is to achieve full understanding of the three dimensional behaviour of the structure and to derive suitable statutes for National Standards.

RÉSUMÉ

Un système de surveillance moderne sera installé sur le pont de Kao Ping Hsi à Taiwan, afin de recueillir et analyser des informations sur le comportement de ce pont pendant des typhons et tremblements de terre, fréquents dans cette région. Le but final de ce projet est de construire des ouvrages encore plus sûrs et de contribuer à l'amélioration des normes nationales.

ZUSAMMENFASSUNG

Es wird an der Kao Ping Hsi Brücke in Taiwan ein innovatives Ueberwachungssystem installiert, das Daten über das Verhalten der Brücke unter den häufig vorkommenden Taifunen und Erdbeben aufzeichnen und analysieren soll. Das Endziel ist es, bessere und sicherere Bauwerke zu entwerfen. Die Ergebnisse sollen in die einschlägigen Bestimmungen der nationalen Normen eingearbeitet werden.

1. THE BRIDGE

The Kao Ping Hsi Bridge in Taiwan is a Cable Stayed bridge with a record breaking cantilever of 330 meters. The overall concept of the bridge is innovative and trend setting. The cross section is a closed steel box, designed to withstand extraordinary dynamic loads. The deck height is 3,20 meters with a width of 34,50 meters and suspended in the middle plane.
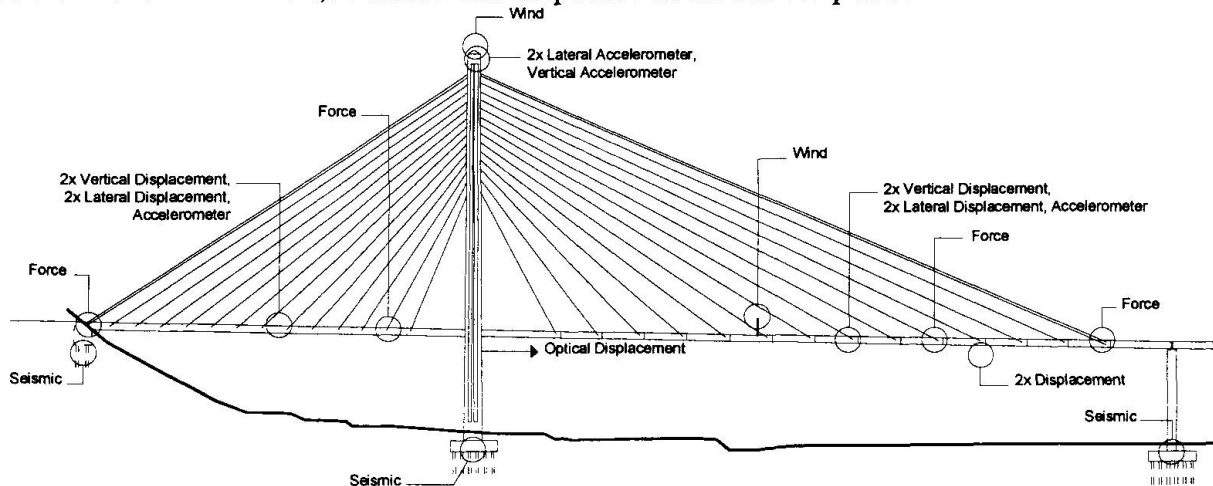
Fig. 1   Kao Ping Hsi Bridge, Taiwan

1.1 The Load Conditions in Taiwan

The island experiences an average of 2 typhoon landings per year. It also receives a total of 65 earthquakes per year, with high potential of a big one within a 60 year return period, that is within the lifetime of the bridge.

The hourly wind speed was determined to be 52 m/sec at deck level, which is 45 m above ground. The peak gust is 76 m/sec with a duration of 4 sec. These loads were determined with the help of a Monte Carlo Simulation considering the 105 typhoons, which have passed through the area within the last 60 years. Turbulence should be below 5% due to the proximity of the sea. A clear Vortex Shedding phenomena was typical recorded with a wind speed of approximately 10 m/sec.

At a nearby recording station, the seismic record shown in Fig. 3 was recently recorded. There have been a considerable number of similar records by this station, over the last 30 years, of the magnitude illustrated in the figure. Therefore it is highly probable that within a reasonable period the response of the bridge during an earthquake will be measured.
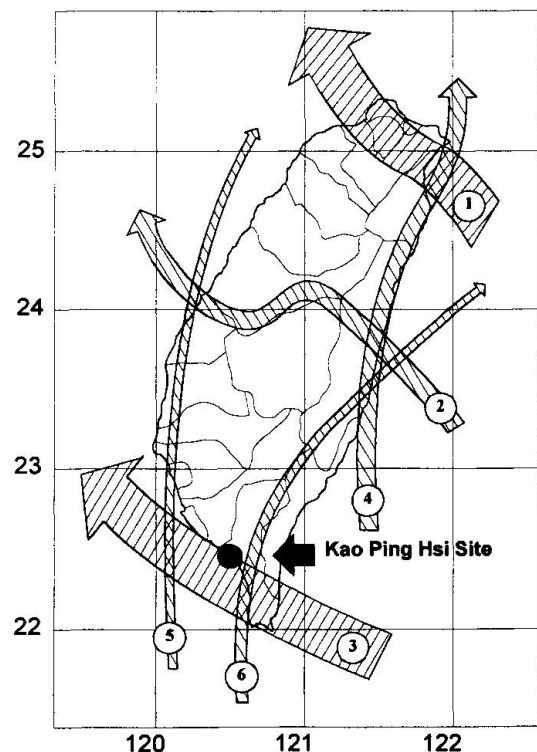
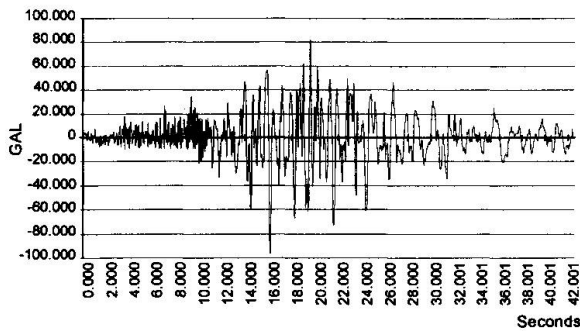**Fig. 2**   Paths of typhoons over Taiwan

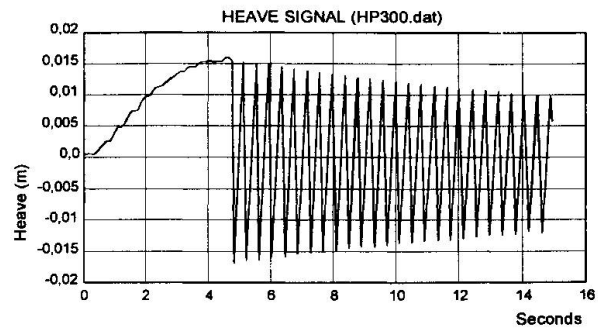**Fig. 3** Seismic event recorded in site area

Fig. 4 Bridge damping characteristic

2. THE MONITORING SYSTEM

2.1 The General Concept

In the future, this Monitoring System shall form a basis for research on Cable Stayed Bridge behaviour under wind and seismic loads. The high probability of a recordable event makes the project most interesting. Therefore a number of Universities, Consultants and Bridge Owners are concentrating to make the project successful.

It was clearly demonstrated by the earthquakes in Los Angeles 1994 and Kobe 1995, that simplifications in modelling and calculation, as applied to date are not able to describe the action sufficiently. The Monitoring System must therefore be able to produce data fulfilling the following criteria:

• Three dimensional recording.
• Recording of the differential motion at all supports.
• Recording of all data that might be of influence on the structural behaviour.

The author is of the opinion that only a full three dimensional analysis will be able to realistically describe the response of the structure due to excitation from wind or earthquake.

2.2 Components of the Monitoring System

To receive complete records the following data are acquired:

• Ground motion in three locations.
• Acceleration of deck and pylon.
• Cable forces of significant cables.
• Displacement of the structure.
• Full meteorological data set.

A sketch of the system is shown in Fig. 5. The system will be implemented step by step, beginning during construction, to receive data about the construction history.
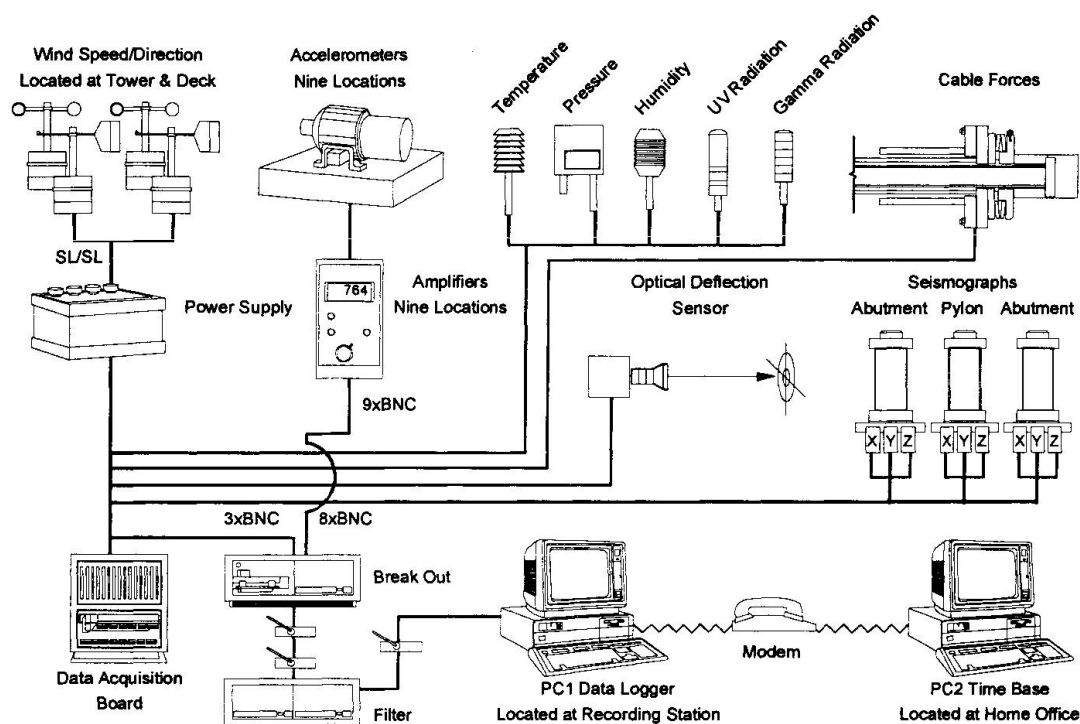
Fig. 5   Monitoring system diagram

2.3   Details of the Sensors

The variations of the cable forces during vibration, as well as temperature changes and traffic loads, are monitored through simple devices that have been developed for this purpose. High quality metal rings will be placed below the cable anchor on top of the pylon. To obtain the best results, each ring has 12 special strain gauges mounted concentricly around it. Relatively weak signals from each strain gauge will be amplified and transmitted up to 500 m, to the location of the data acquisition unit.

The data acquisition unit represents an intelligent system designed to receive analog signals.

Fig. 6   Cable forces sensor
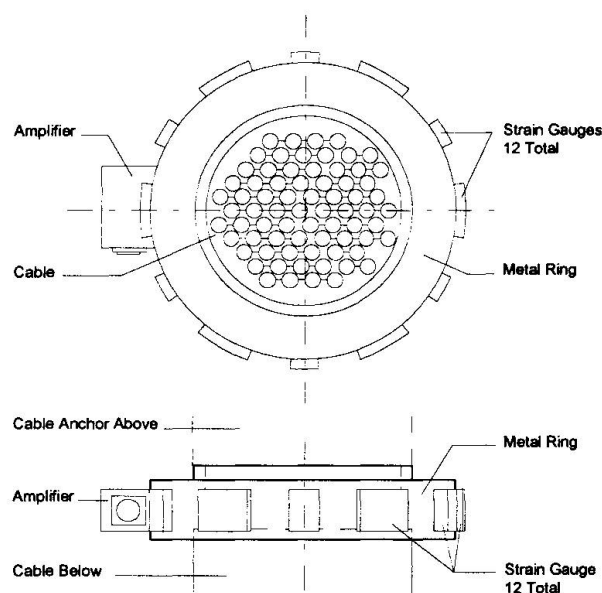
The measurement of acceleration of the structure is performed in correlation with the measurements from the full model wind tunnel test. This will allow a direct comparison of results and provide information on the reliability of the test. To support the results from the acceleration measurement, an optical displacement instrument will be installed. It consists of a laser controlled

deflection measurement unit. This will allow data from different sources, which should conform, to be compared.

The wind recording shall enable the engineers to define the wind profile at the location of the bridge and generate data about turbulence and coherence of the wind field. This is particularly important, since these types of measurements are not currently available in Taiwan.

2.4 Data Recording Unit

For data recording, analysis and control, an integrated multi-synchronous channel system was chosen. This system allows on-line or time controlled conditioning of the signals from the sensors by amplifiers, filters or counters. The data can be recorded simultaneously and are transferred to an event recorder, which can be freely programmed to suit the requirements. The system might be also used as data logger or printer.

The sampling rate for the accelerometers is 100 Hz, which generates huge quantities of data. A selection process was designed to record considerable events only. The basic concept is:

- To record any event that reads above a predetermined target value.
- To record major events and their history dated back at least 48^h to find out if there is any visible indication in the data on the force of the coming event.
- A customer defined program segment shall enable the user to record in any other mode.

The data shall be transferred via modem to a PC, where the data are processed. The program is installed under "Windows", which makes the application easy and comfortable to use. The data are controlled by powerful macros, which provide comfort and flexibility in the handling of the system. It allows:

- Comfortable adjustment of the measurements by the recording unit.
- Automatic data transfer from the logger to the PC.
- Triggering of measuring programs on customer's requirement.
- On-line display of any channel required.
- Data reduction and compression to save storage space.
- Control of complex measurement programs by way of synthesizer, controller and digital input/output.

2.5 Data Processing

The main target is to find a relevant spectrum for seismic activities in the area and to confirm the accuracy of the results of the wind tunnel tests. The quality of the results will be highly dependent on the number of readings available. The various earthquake recordings will be superimposed to find similarities.

Typical examples are the detection of Vortex Shedding excitation as determined in the wind tunnel tests. Refer to Fig.7. The target is to close the gap between wind tunnel results and the very rare site measurements. Another interesting result would be real figures for the damping of the structure. A typical vibration is shown in Fig.4, which represents the response after an impact.
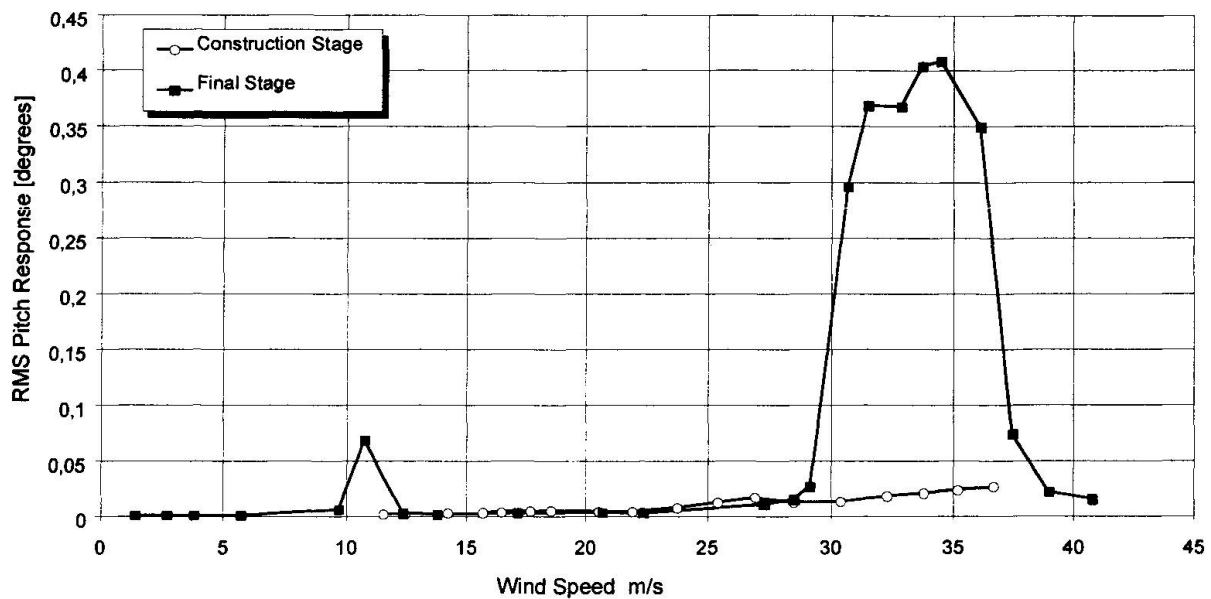
Fig. 7   Predicted vortex shedding excitation

3. CONCLUSION

The proposed Monitoring System will produce data that will help structural engineers understand their structures and arrive at realistic loading conditions for extraordinary structures. The proposed Monitoring System shall fulfil all requirements of flexibility and interactive control to react on recorded events. It is intended to take a step forward in bridge engineering for countries with high risk potential.

REFERENCES:

1. DAVENPORT A.G., The Relationship of Wind Structure to Wind Loading. National Physical Laboratory, Teddington, London. Her Majesty's Stationery Office, 1965.
2. GIMSING Prof. Niels J., Cable Supported Bridges: Concept and Design. Gimsing, 1983.
3. RHIE Seungu R., New Bridge Types for Long Spans. Springer-Verlag. Vienna. New York, 1993.
4. WENZEL Dr., H. Cable-Stayed Bridge in a Typhoon Area: Interaction Between Construction Technology and Design. IABSE Symposium. Leningrad, 1991.

Acoustic Emission Monitoring of Bridges under Heavy Truck Loading
Surveillance par émissions acoustiques de ponts surchargés
Kontrolle der überlasteten Brücken unter Verwendung der akustischen Emission
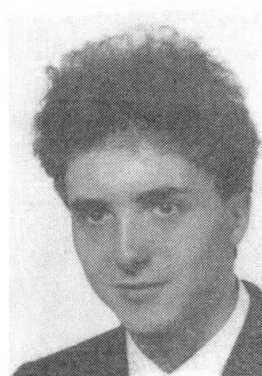
Przemystaw MALISZKIEWICZ
Assistant Professor
Technical University of Wroclaw
Wroclaw, Poland

Przemystaw Maliszkiewicz, born in 1954, received his civil engineering degree at WTU. He is involved in non destructive evaluation methods for the diagnosis of bridges.

Daniel ANTONIAK
Assistant Professor
Technical University of Wroclaw
Wroclaw, Poland

Daniel Antoniak, born in 1968, received his civil engineering degree at WTU, where he is a doctoral candidate studying the modelling of prestressed concrete structures.

SUMMARY

The paper reports test results of acoustic emission monitoring of two bridges under heavy truck loading. Measurement of the signals is compared with the results of calculation. Application of the acoustic emission as the method for early warning during passage of the vehicle along the bridge is shown in the paper. Post-test assessment of the stresses of structural members under heavy loading in comparison to the acoustic emission measured for normal traffic is presented.

RÉSUMÉ

L'article présente les résultats d'auscultation de deux ponts routiers à l'aide d'une méthode d'émission acoustique. Les mesures d'émission acoustique ont été comparées avec les résultats des calculs numériques. L'application d'émission acoustique ainsi que la méthode de la prévention pendant les passages des véhicules dépassant les charges admissibles sont présentées. La méthode permet d'évaluer les efforts dans les éléments de construction sous la charge d'une circulation routière normale.

ZUSAMMENFASSUNG

Im Aufsatz wurden die Ergebnisse der stetigen Kontrolle von zwei übernormativ belasteten Brücken mit der Verwendung der akustischen Emission vorgestellt. Diese Messungen wurden mit den Ergebnissen der Berechnungen verglichen. Vorgestellt werden die Verwendung der akustischen Emission als die Methode des frühzeitigen Warnens während übernormativen Überfahrten. Die Methode erlaubt de Bestimmung der Belastung der Konstruktion unter normaler Verkehrslast.

1. INTRODUCTION

Evaluation of the bridge structure subjected to special multiaxial vehicles for carrying of heavy equipment as machinery, transformer elements, etc. is very difficult problem for bridge maintenance service. Preliminary calculations of loading capacity and displacements of a structure, especially for old bridges, must be done prior to the passage of the vehicle of this type. Acoustic Emission (AE) measurement is the technique which enables monitoring of the behavior of the structure elements under loading. It seems to be efficient tool for early warning against damage of the structure members under heavy vehicles loading.

2. DESCRIPTION OF TESTED STRUCTURES

2.1. Bridge I

It is a steel three span (60.0+84.0+60.0 m between supports) road bridge over the West Odra river. The main construction consists of four double–tee section girders of 2.90 m spacing. The girders are divided by hinges into one secondary span of length 75.0 m and two cantilever spans 54.0 m long.

2.2. Bridge II

The superstructure of the bridge over the Noteć river consists of two truss girders of triangular type with 6.0 m spacing between the girders. The deck is composed of transverse and longitudinal beams. The span of the bridge is 52.2 m. Sidewalks are placed on cantilevers outside truss girders.

3. GENERAL ASSESSMENT OF TECHNICAL STATE OF STRUCTURES

The principal aim of the conducted tests was determining the ability of the bridges to carry heavy truck loading.

The evaluation of technical state is based only on observation done during the measurements and can be summarized as follows:
- bridges I exhibits significant vibrations under service load,
- no significant damage of spans and supports of bridges I was observed,
- main girders of *bridge II* are in good condition,
- the superstructure of *bridge II* seems to be insufficiently stiff.

4. TESTING PROGRAM

Four stages of testing program can be distinguished. These are:
- initial measurements of AE of mostly loaded elements of the structures under service load,
- measurements of AE under service load just before loading with heavy truck,
- measurements of AE under heavy truck load,
- static analysis in the range enabling evaluation of the AE level under real load.

Measurements of acoustic emission were carried out continuously for common traffic with different weights and technical characteristics of vehicles, random frequencies of load appearance, and variable speed of vehicles. During initial tests several 5 up to 15 minute measurements were done. In some cases the instant of vehicle appearance on a bridge and vehicle movement direction were registered.

The heavy truck moved very slowly (about several meters a minute) along the middle of bridge roadway. In order to avoid serious damage of a bridge constant monitoring of chosen measurepoint was carried out which would signal overloading by fast and unstable increase of AE rate. During crossing of the secondary span of *bridge I* the truck was stopped for some tens of seconds.
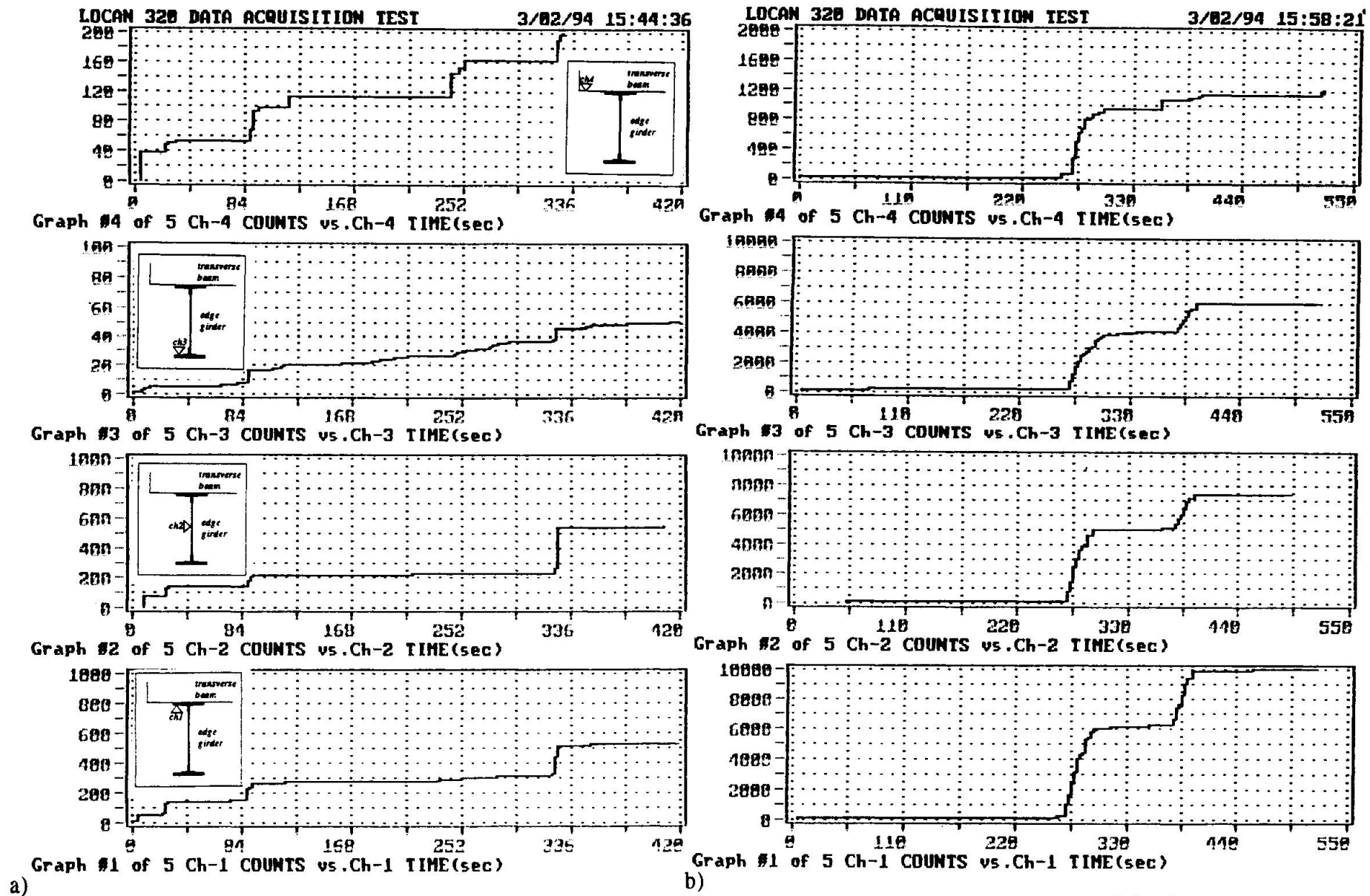
Graph #4 of 5 Ch-4 COUNTS vs.Ch-4 TIME(sec)

Graph #3 of 5 Ch-3 COUNTS vs.Ch-3 TIME(sec)

Graph #2 of 5 Ch-2 COUNTS vs.Ch-2 TIME(sec)

Graph #1 of 5 Ch-1 COUNTS vs.Ch-1 TIME(sec)

a)

Graph #4 of 5 Ch-4 COUNTS vs.Ch-4 TIME(sec)

Graph #3 of 5 Ch-3 COUNTS vs.Ch-3 TIME(sec)

Graph #2 of 5 Ch-2 COUNTS vs.Ch-2 TIME(sec)

Graph #1 of 5 Ch-1 COUNTS vs.Ch-1 TIME(sec)

b)

Fig.1 Comparison of number of AE counts measured for the *bridge I*, a) under service load, b) under heavy truck load

P. MALISZKIEWICZ, D. ANTONIAK

227

5. EQUIPMENT

Measurements of AE were obtained with the use of LOCAN 320 system made by Physical Acoustic Corporation in Princeton. LOCAN 320 is a computer aided system for measuring and acquisition of acoustic emission signals in real time. The signals of high frequencies are emitted by a loaded structure and then transformed into electric signals by piezoelectric transducers.

6. TEST RESULTS

Test results from measurement of AE signals generated by *bridge I* members are shown in Fig. 1 AE structure response under service load was compared with the signals emitted by the same members under passage of the heavy vehicle. Measurements were done with amplification of 40 dB and "floating threshold" 25 dB.

Measurements of AE for *bridge II* were done with following levels of amplification and discrimination:
- ch1 – amp. 30 dB, thresh. 40 dB,
- ch2 – amp. 30 dB, thresh. 30 dB,
- ch3,4 – amp. 24 dB, thresh 51 dB.

Test results for monitoring of the *bridge II* subjected to heavy truck loading is shown in Fig.3

7. CONCLUSIONS

The analysis of obtained results yields following conclusions grouped for service and heavy truck load.

7.1. Test results for service load

- each crossing of vehicles produces acoustic emission at monitored construction elements,
- in the *bridge I* the most emission was obtained in the web and compressed flange of main girder; in the case of dynamic load a part of AE signal can be caused by allowances, friction and knocks of deck elements at top flange of girder,
- low amplitudes (below 30 dB) of most acoustic emission registered under service load of *bridge I* point at friction as the source of signals, whereas in *bridge II* emission consists of signals of high amplitudes 40÷60 dB, 30÷70 dB and 50÷80 dB for bottom flange of truss, transverse beam and diagonal bar of truss respectively,
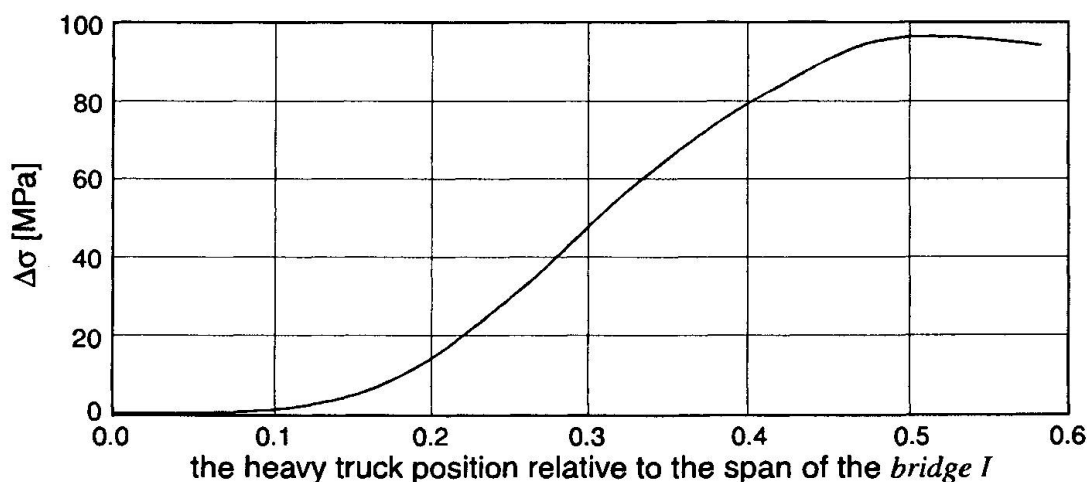

Fig. 2. Increase of maximal normal stress in the transverse beam of *bridge II* during the passage of the heavy truck
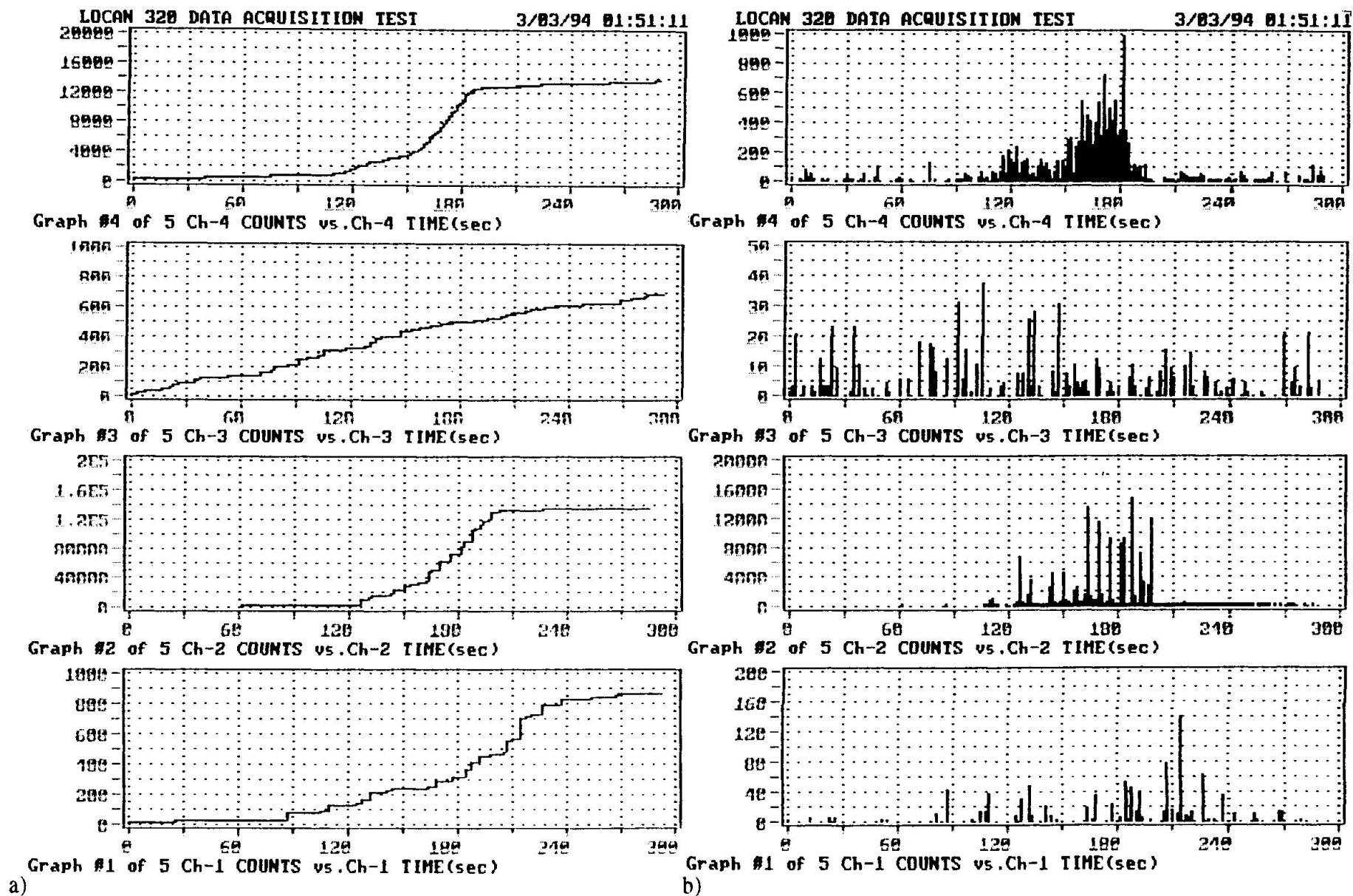
Graph #4 of 5 Ch-4 COUNTS vs.Ch-4 TIME(sec)

Graph #3 of 5 Ch-3 COUNTS vs.Ch-3 TIME(sec)

Graph #2 of 5 Ch-2 COUNTS vs.Ch-2 TIME(sec)

Graph #1 of 5 Ch-1 COUNTS vs.Ch-1 TIME(sec)

a)

Graph #4 of 5 Ch-4 COUNTS vs.Ch-4 TIME(sec)

Graph #3 of 5 Ch-3 COUNTS vs.Ch-3 TIME(sec)

Graph #2 of 5 Ch-2 COUNTS vs.Ch-2 TIME(sec)

Graph #1 of 5 Ch-1 COUNTS vs.Ch-1 TIME(sec)

b)

P. MALISZKIEWICZ, D. ANTONIAK

Fig.3 Comparison of number of AE counts (a) and AE rate (b) measured for the *bridge I* I under heavy truck load; ch1 −bottom chord of the truss, ch2 −transverse beam, ch3,4 − truss diagonals

229

acoustic emission level measured in *bridge II* regardless of less intensity of loading is significantly higher than in *bridge I*, especially high level was observed in the middle transverse beam of *bridge II* (sum of AE signals is an order higher than measured in bottom flange and diagonals).

Bridge	Element	Maximal normal stress [MPa]		
		Dead weight	Service load	Heavy truck load
bridge I	edge girder (ch 1,2,3)	97	18	32
	transverse beam (ch 4)	26	21	84
bridge II	bottom chord of truss (ch1)	125	23	42
	transverse beam (ch2)	107	44	96
	diagonal (ch3)	130	33	61
	diagonal (ch4)	158	51	94

Table 1. Maximal calculated stresses in bridge elements

7.2. Test results for heavy truck load

Measurements of AE signals during passage of heavy truck along tested bridges enabled following conclusions to be drawn.

7.2.1 Bridge I

• AE was registered after the truck got to the secondary span indicating that friction in hinges was not the source of emission,

• the stopping of the truck during the passage along the bridge was accompanied by stabilization of number of AE counts (see fig. 1), especially in the web of the main girder and in transverse beam, in the flanges of the main girders AE rate also decreased, however at this level of loading the stopping of the truck caused exponential decreasing of AE,

• after the stopping further increase of AE is observed as the truck was approaching the middle of the bridge,

• the level of AE caused by heavy truck loading is an order higher than the one obtained for single vehicles in common traffic; numbers of AE counts measured in web, top and bottom flange of main girder are in the same range what shows similar effort of these elements; the number of counts registered in transverse beam is several times lower.

7.2.2 Bridge II

• the heavy truck loading produced significant acoustic effect especially in transverse beam (Fig. 3, channel 2); when the truck went on the bridge acoustic emission of rapidly increasing number of counts (up to $1.4 \cdot 10^5$) appeared; such a level of emission may indicate overloading of structure element and possibility of serious damage,

• it is significant the AE rate increases with growth of applied loading (see *bridge I*, Fig. 1),

• AE signal decreased quickly after the truck went off the bridge but the signal lasted still about 100 seconds at the level of tens of counts a second,

• during the heavy truck passage amplitudes of registered signals were similar to those obtained under service load what implies that the source of AE signals was the same,

• significant increase of AE was observed in a diagonal of the truss as the truck went on the bridge,

• relatively small effort was registered in the bottom chord of the truss; the number of AE counts is comparable to that obtained with service load.
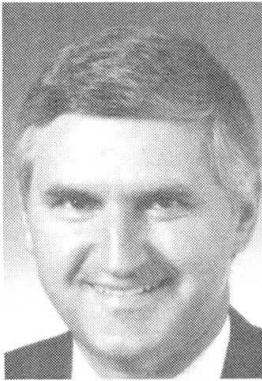
Monitoring Bridge Load Spectra
Mesure des charges sur les ponts
Messungen von Brückenlasten

Andrzej S. NOWAK
Professor
University of Michigan
Ann Arbor, MI, USA

Andrzej S. Nowak received his Ph.D. from Warsaw Univ. of Technology, Poland, and has been at University of Michigan since 1979. He has been involved in reliability-based development of the LRFD bridge design codes in the United States and Canada.

Jeffrey A. LAMAN
Research Associate
University of Michigan
Ann Arbor, MI, USA

Jeffrey Laman recently completed his Ph.D. at the University of Michigan. His dissertation focused on fatigue load models for girder bridges. For the past four years he has been conducting tests on steel highway bridges. He also has ten years of professional engineering experience.

SUMMARY

The objective of the study is to determine actual live loads for highway bridges located within a large metropolitan area. Truck weights were measured using weight-in-motion technology. The parameters obtained include gross vehicle weight, axle weights and axle spacing. Seven bridges were selected to represent the total population. The statistical data is presented as cumulative distribution functions. The results are shown for the different parameters. Live load varies considerably from site to site.

RÉSUMÉ

L'objectif de cette étude est de déterminer les charges réelles sur les ponts. Les paramètres considérés sont le poids et la dimension des camions. Sept ponts sont étudiés. Les résultats sont présentés sous forme de fonctions statistiques.

ZUSAMMENFASSUNG

Das Ziel dieses Projekts ist die Bestimmung von Brückenlasten. Die untersuchten Parameter sind Gewichte und Dimensionen von Lastwagen. Insgesamt wurden sieben Brükken ausgesucht. Die Ergebnisse werden anhand von statistischen Funktionen dargestellt.

1. INTRODUCTION

The two major questions facing bridge owners are: what is the actual strength of the structure and what is the remaining life? Structural performance depends on bridge resistance and actual loads. It has been observed that truck loads are strongly site-specific. There is considerable variation in traffic volume and truck weights, even within a given geographic area. Therefore, the objective of this paper is to present actual truck loads on selected bridges in a major metropolitan area.

Seven bridges were selected to represent a wide cross section of traffic in the greater Detroit area. The selection criteria included location, accessibility for testing equipment, span length, truck traffic volume and presence of traffic control. The basic parameters of the selected bridges are summarized in Table. 1. The parameters include span length, number of girders, girder spacing, number of traffic lanes and average daily truck traffic (ADTT).

Table 1. Parameters of Selected Bridges.

No.	Symbol	Span (m)	Number of girders	Girder spacing (m)	Number of lanes	ADTT (one direction)
1	WY/I94	10	9	1.55	2	750
2	I94/M10	33	5	2.70	2	1,500
3	US12/I94	12	9	1.65	2	500
4	DA/M10	13	8	1.60	2	750
5	M39/M10	10	8	1.85	3	1,500
6	I94/I75	13.5	8	1.40	2	1,500
7	M153/M39	9.5	12	1.75	3	500

Measurements were taken using a weigh-in-motion (WIM) system. The truck weights and axle weights are calculated from strains measured in bridge girders. Sensors were installed in each lane at the bridge entrance to determine the vehicle speed, number of axles and axle spacing. The equipment is calibrated using a truck with known axle weights. Measurement accuracy of gross vehicle weight (GVW) is about 5 percent for most types of trucks and the measurement accuracy of axle weights is about 20 percent. Selected bridges were instrumented and measurements were taken for two or three consecutive days.

2. TRUCK TRAFFIC

The number of axles on trucks varies. Analysis of the WIM data indicates that a majority of the trucks are two axle vehicles. Many two axle vehicles are of low GVW and do not affect the bridge life. An important vehicle type is the five axle truck, which is the majority of the heavier vehicles (greater than 70 kN). The heaviest vehicles in the Detroit Metropolitan Area are 11 axle trucks,

which constitute up to five percent of truck traffic with GVW greater than 70 kN.

The general observation that live load on bridges is strongly site-specific can be made from the WIM data. There is a considerable variation in traffic volume and weight of trucks from sit to site. The estimated average daily truck traffic (ADTT) (in one direction) varies from 500 to 1,500. The maximum observed truck weight varies from 350 kN to 1,100 kN. The maximum observed axle weights vary from 90 kN to nearly 220 kN. The largest GVW and axle weights were observed on interstate highway I-94 and Michigan highway M-39. These roads also have the largest observed traffic volume with an estimated ADTT of 1,500 in each direction. The weight of trucks on surface roads with lower volume of traffic is mostly within the legal limits.

3. TRUCK WEIGHTS AND AXLE WEIGHTS

Results of field truck measurements are shown on normal probability paper. The vertical axis is the inverse of the standard normal probability function, corresponding to the probability exceedance. For example, 0 corresponds to probability 0.5 and 2 corresponds to 0.02 (the probability of exceeding given value of truck weight is 0.02).

The CDFs of GVW are plotted in Fig. 1. The observed extreme GVW varies depending on the route. Most overloaded trucks were observed on I-94 and M-39, which are high volume highways. For these two bridges, the maximum GVWs are approximately 1,000 kN. For other bridges, the maximum values of GVW are approximately 700 kN.
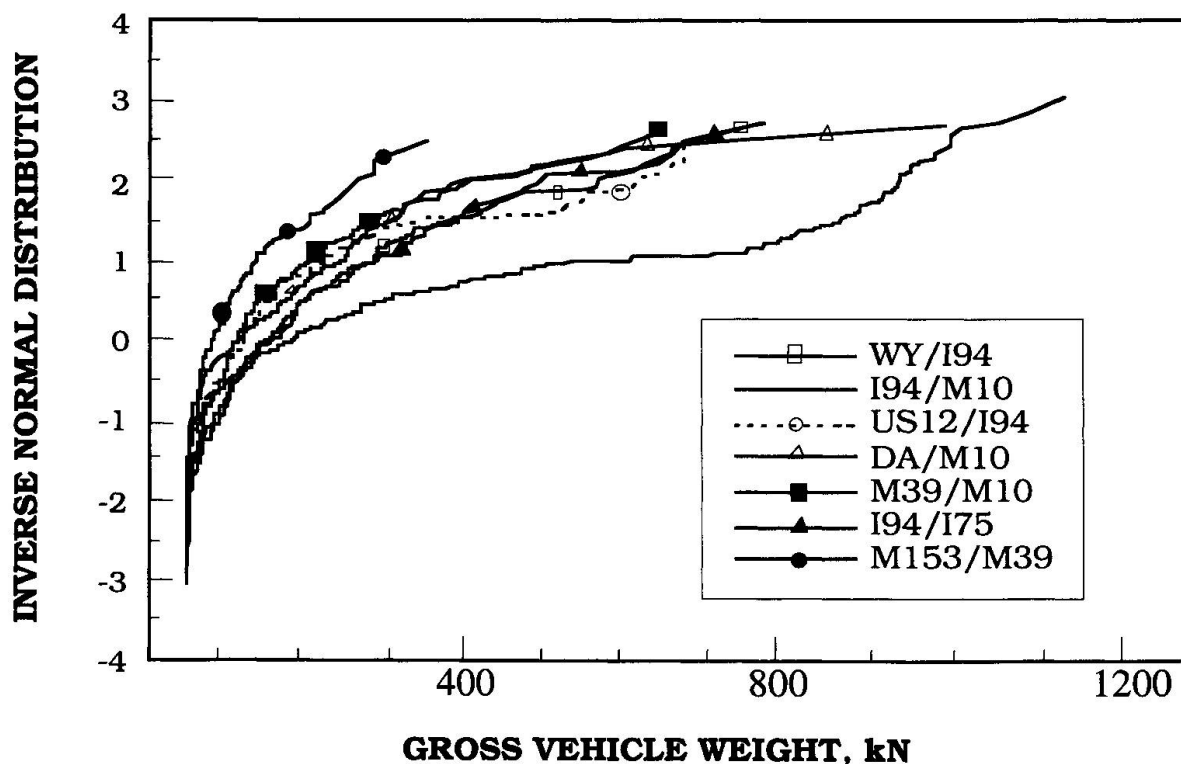

Fig. 1. Distribution Functions of Gross Vehicle Weight.

Truck axle weight is also an important parameter. The CDFs of axle weight are shown in Fig. 2 for the considered bridges. Similar to the GVW, the extreme values are associated with bridges carrying I-94 and M-39. The largest values of axle weight exceed 200 kN.
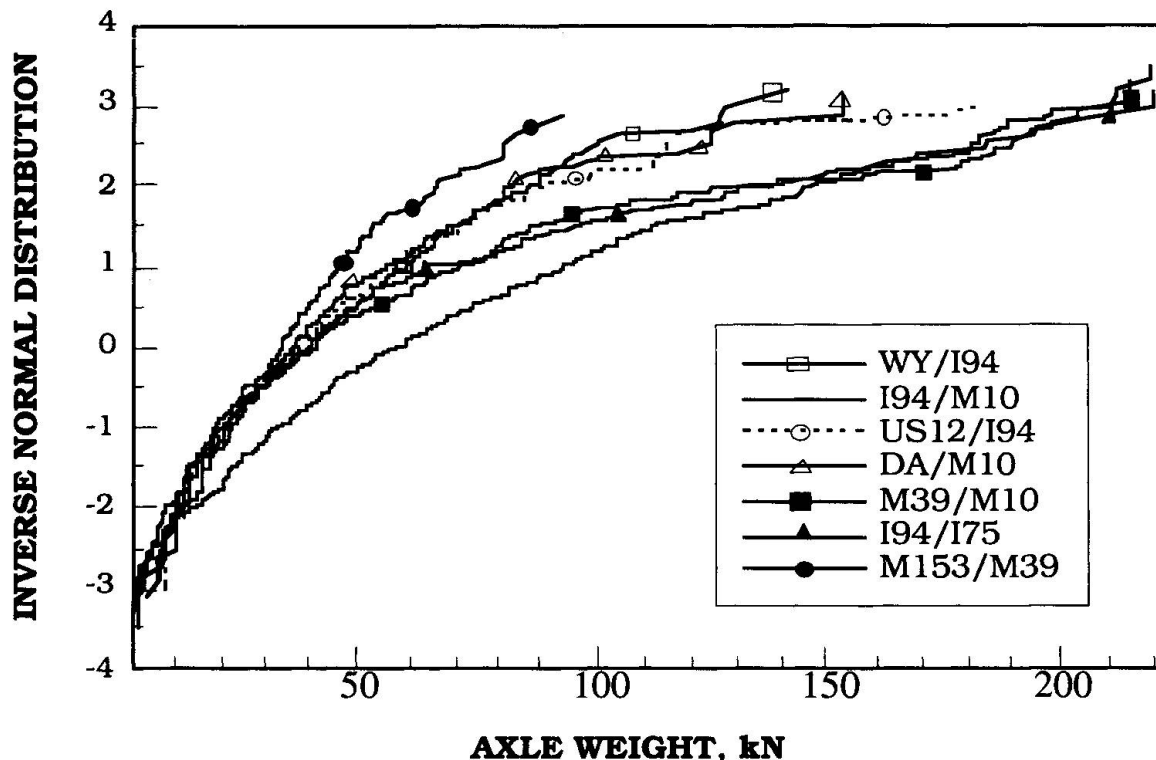

Fig. 2. Distribution Functions of Axle Weight.

4. EFFECT OF BRIDGE LIVE LOAD

Bridge damage is caused by load effect rather than the load itself. The effect of truck loads on bridges can be evaluated by consideration of lane moments. The calculations were carried out using influence lines. The maximum simple span moment was determined for each truck in the data base. The results are shown in Fig. 3 on normal probability paper. For an easier comparison, the moments are divided by corresponding HS-20 moments, calculated according to the AASHTO Specifications (1992).

The variation of maximum moments is similar to that of gross vehicle weights. For I-94 and M-39, the extreme values exceed 2.5 HS-20 moments. For other bridges, the maximum moments are about 1.5 design live load.

To determine the actual load taken by each girder, stress spectra were determined using the rainflow method. It was observed that even though a large number of trucks exceed the legal weight limits, the actual stress range due to live load is within acceptable limits. However, the number of axle weights exceeding the legal limits seems to be too high. Multiple passages of heavy axles contribute to the deterioration of the bridge deck slabs and road pavement. More law enforcement may be needed for the highways with a high percentage of overloads.
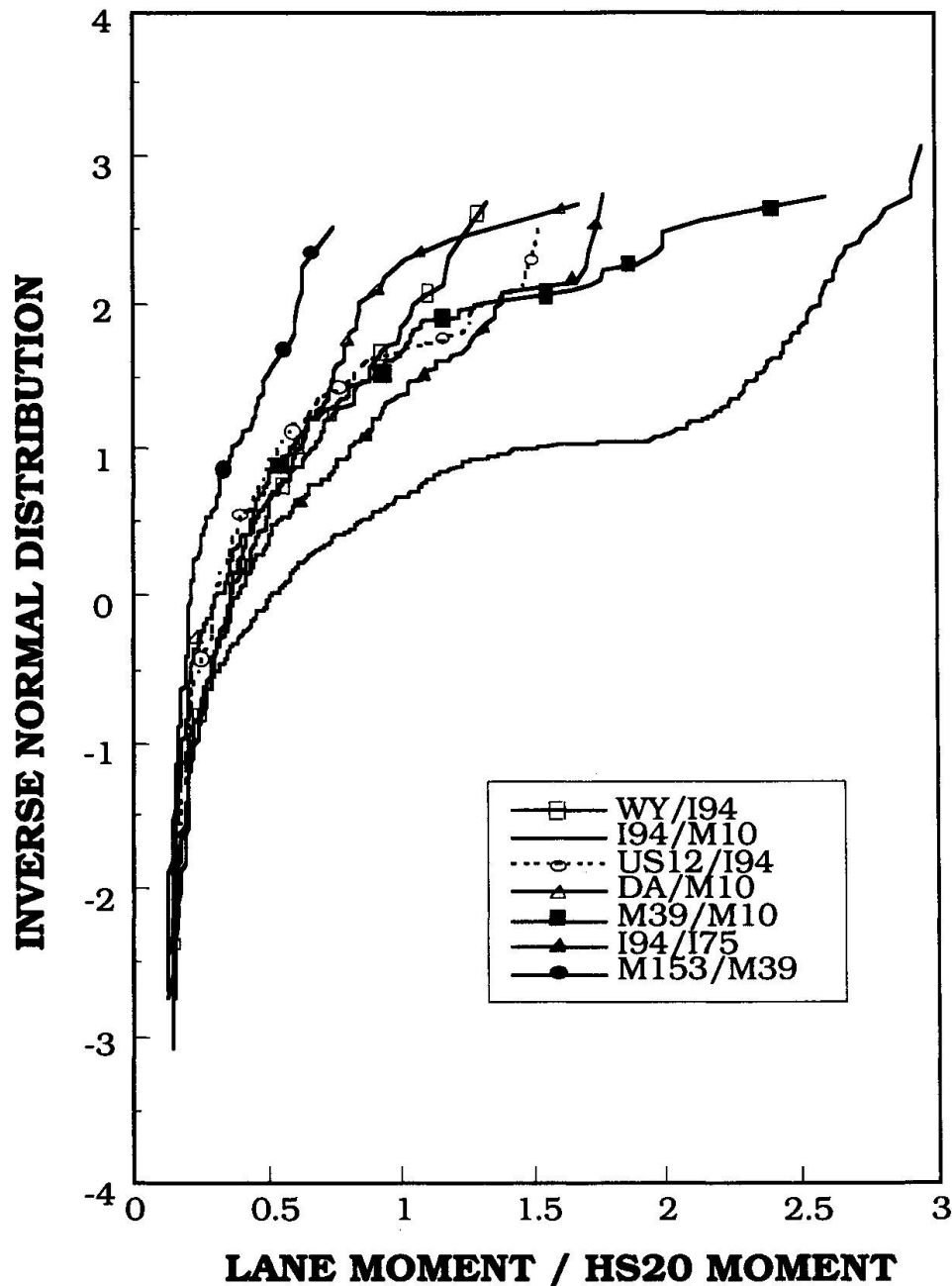
Fig. 3. Distribution Functions of Midspan Moments.

6. CONCLUSIONS

The tests were carried out on bridges located on various types of roads in the Metropolitan Detroit Area. Some of these bridges carry surface street traffic while others carry highway loads. The results of measurements indicate that traffic is strongly site-specific. This applies to number of trucks, gross vehicle weight, axle weight and midspan moment.

REFERENCES

Laman, J.A., "Fatigue Load Models for Girder Bridges", Doctoral Dissertation, University of Michigan, Ann Arbor, Michigan, January 1995.

Laman, J.A., "Load Spectra for Girder Bridges", Fourth International Bridge Engineering Conference in San Francisco, CA, TRB, Washington. D.C., August 1995, to appear.

Laman, J.A. and Nowak, A.S., "Verification of Truck Loads for Girder Bridges", ASCE, Structures Congress, Boston, MA, April 1995, to appear.

Nowak, A.S., Kim, S., Laman, J.A., Saraf, V. and Sokolik, A. F., "Truck Loads on Selected Bridges in the Detroit Area", Research Report UMCE 94-34, Department of Civil and Environmental Engineering, University of Michigan, Ann Arbor, Michigan, December 1994.

Nowak, A.S., Laman, J.A. and H. Nassif, "Effect of Truck Loads on Bridges", Research Report UMCE 94-22, Department of Civil and Environmental Engineering, University of Michigan, Ann Arbor, Michigan, October 1994.